the TSC genes and the *PTPN11* gene are likely to contribute to the development of ASDs in patients with these syndromes.

NF-I is well known to be associated with ASDs. The prevalence of autism in patients with NF-I was reported to be 4% [9]. The well-known function of the NF-I protein is to act as a RAS-GTPase-activating protein known to be involved in the regulation of the RAS-mitogen-activated protein kinase (MAPK) pathway. Mutations in the NF-I gene are thought to result in activation of the RAS/MAPK signal transduction pathway [2]. Clinical overlap between LEOPARD syndrome and NF-I is also well known [19].

Approximately 50% of patients with Noonan syndrome are due to missense *PTPN11* mutations [20]. *PTPN11* encodes SHP2, a protein tyrosine phosphatase, that is involved in the activation of the RAS/MAPK cascade [2]. Noonan syndrome is caused by "gain of function" *PTPN11* mutations [1,2], and the SHP2 mutants due to the *PTPN11* mutations causing Noonan syndrome cause prolonged activation of the RAS/MAPK pathway [2]. Schubbert et al. [21] reported that germline KRAS mutations cause Noonan syndrome through the hyperactive RAS/MAPK pathway.

Herault et al. [22] reported a positive association of the HRAS gene and autism. The psychological profiles of adults and children with Noonan syndrome have been studied, and deficiencies in social and emotional recognition and expression have been identified in adults, while low verbal IQ, clumsiness, and impairment of developmental coordination have been reported in children [23].

To date, there have been no reports to suggest an association of LEOPARD syndrome and ASDs. Our observations in this familial case may suggest at least some degree of association between LEOPARD syndrome and ASD phenotypes possibly through the RAS/MAPK signal transduction pathway. Further studies with more patients with LEOPARD syndrome are needed to establish the association and to investigate the genetic contributing factors causing ASDs, leading to the prevention and earlier detection of ASDs and better management of patients with these disorders.

References

[1] Kontaridis M, Swanson KD, David FS, Barford D, Neel BG. PTPN11 (Shp2) mutations in LEOPARD syndrome have dominant negative, not activating, effects. J Biol Chem 2006;281: 6785–92.

[2] Aoki Y, Niihori T, Narumi Y, Kure S, Matsubara Y. The RAS/MAPK syndromes:novel roles of the RAS pathway in human genetic disorders. Hum Mutat 2008;29:992–1006.

[3] Wing L. Autistic spectrum disorders. BMJ 1996;312:327–8.

[4] Khouzam HR, El-Gabalawi F, Pirwani N, Priest F. Asperger's disorder: a review of its diagnosis and treatment. Comp Psychiatr 2004;45:181–91.

[5] American Psychiatric Association. Diagnostic and Statistical Manual of Mental Disorders. 4th ed.-Text Revision. Washington, DC: American Psychiatric Association; 2000.

[6] Muhle R, Trentacose SV, Rapin I. The genetics of autism. Pediatrics 2004;113:e472–86.

[7] Curatolo P. Tuberous sclerosis: genes, brain, and behavior. Dev Med Child Neurol 2006;48:404.

[8] Gillberg C, Forsell C. Childhood psychosis and neurofibromatosis-More than a coincidence? J Autism Dev Disord 1984;14: 1–8.

[9] Williams PG, Hersh JH. The association of neurofibromatosis Type 1 and autism. J Autism Dev Disord 1998;28:567–71.

[10] Cohen IL, Sudhalter V, Pfadt A, Jenkins EC, Brown WT, Vietze PM. Why are autism and the fragile-X syndrome associated? Conceptual and methodological issues. Am J Hum Genet 1991;48:195–202.

[11] Verhoeven W, Wingbermuhle E, Egger J, Van der Burgt I, Tuinier S. Noonan syndrome: psychological and psychiatric aspects. Am J Med Genet A 2008;146A:191–6.

[12] Ghaziuddin M, Bolyard B, Alessi N. Autistic disorder in Noonan syndrome. J Intell Disabil Res 1994;38:67–72.

[13] Niihori T, Aoki Y, Ohashi H, Kurosawa K, Kondoh T, Ishikiriyama S, et al. Functional analysis of PTPN11/SHP-2 mutants identified in Noonan syndrome and childhood leukemia. J Hum Genet 2005;50:192–202.

[14] Ehlers S, Gillberg C, Wing L. A screening questionnaire for Asperger syndrome and other high-functioning autism spectrum disorders in school age children. J Autism Dev Disord 1999;29:129–41.

[15] Wahlstrom J, Gillberg C, Gustavson KH, Holmgren G. A Swedish multicenter study. Am J Med Genet 1986;23:403–8.

[16] Tranebjaerg L, Kure P. Prevalence of fra (X) and other specific diagnoses in autistic individuals in a Danish county. Am J Med Genet 1991;38:212–4.

[17] Ke Y, Zhang EE, Hagihara K, Wu D, Pang Y, Klein R, et al. Deletion of Shp2 in the brain leads to defective proliferation and differentiation in neural stem cells, and early postnatal lethality. Mol Cell Biol 2007;27:6706–17.

[18] Karbowniczek M, Cash T, Cheung M, Robertson GP, Astrinidis A, Henske EP. Regulation of B-Raf kinase activity by Tuberin and Rheb is mammalian target of Rapamycin (mTOR)-independent. J Biol Chem 2004;279:29930–7.

[19] Sarkozy A, Conti E, Digilio MC, Marino B, Morini E, Pacileo G, et al. J Med Genet 2004;41:e68.

[20] Tartaglia M, Mehler EL, Goldberg R, Zampino G, Brunner HG, Kremer H, et al. Mutations in PTPN11, encoding the protein tyrosine phosphatase SHP-2, cause Noonan syndrome. Nat Genet 2001;29:465–8.

[21] Schubbert S, Zenker M, Rowe SL, Boll S, Klein C, Bollag G, et al. Germline KRAS mutations cause Noonan syndrome. Nat Genet 2006;38:331–6.

[22] Herault J, Petit E, Martineau J, Perrot A, Lenoir P, Cherpi C, et al. Autism and genetics: clinical approach and association study with two markers of HRAS gene. Am J Med Genet 1995;60:276–81.

[23] Lee DA, Portnoy S, Hill P, Gillberg C, Patton MA. Psychological profile of children with Noonan syndrome. Dev Med Child Neurol 2005;47:35–8.

Please cite this article in press as: Watanabe Y et al. A familial case of LEOPARD syndrome associated with a high-functioning autism spectrum disorder. Brain Dev (2010), doi:10.1016/j.braindev.2010.10.006

CLINICAL REPORT

AMERICAN JOURNAL OF medical genetics

Implications of Prenatal Diagnosis of the Fetus With Both Interstitial Deletion and a Small Marker Ring Originating From Chromosome 5

Hiroyasu Ohashi,[1] Kaoru Suzumori,[1,2]* Yasushi Chisaka,[3] Shinichi Sonta,[1] Tomoko Kobayashi,[4] Yoko Aoki,[4] Yoichi Matsubara,[4] Michiko Sone,[5] and Lisa G. Shaffer[6]

[1]Fetal Life Science Center, Ltd., Nagoya, Japan

[2]Department of Obstetrics and Gynecology, Nagoya City University, Nagoya, Japan

[3]Department of Obstetrics and Gynecology, Tohoku University, Sendai, Japan

[4]Department of Medical Genetics, Tohoku University, Sendai, Japan

[5]Kagawa National Children's Hospital, Zentsuji, Kagawa, Japan

[6]Signature Genomic Laboratories, Spokane, Washington

Received 5 May 2010; Accepted 2 August 2010

We describe a patient with 47,XY,del(5)(p11p13), 1 mar observed in prenatal screening. We performed analyses including G-banding, multi-color fluorescent in situ hybridization (mFISH) for fetal chromosome detection. After birth array-based comparative genomic hybridization (aCGH), bacterial artificial chromosome (BAC)-FISH was carried out to define the chromosomal changes precisely. The mFISH revealed that a ring chromosome that had originated from chromosome 5. The aCGH showed that this fetus had a terminal duplication, an interstitial deletion, and a pericentromeric duplication of the short arm of chromosome 5. This complex alteration resulted in partial trisomy 5p15.33–p15.31, partial monosomy 5p14.3–p13.2, and partial trisomy 5p12–p11. To clarify these alterations, we performed BAC-FISH using BAC clones related to deleted and duplicated regions, and found that a derivative (der) chromosome 5 showed the presence of hybridization signals from the duplicated region at 5p15.33 and the loss of hybridization signals from the deleted region at 5p14.2. In addition, FISH analysis confirmed the origin of the marker chromosome. Hybridization signals from the second intervening sequence at 5p13.1, between the deleted region and the pericentric duplicated region, were present on the marker ring chromosome. © 2010 Wiley-Liss, Inc.

Key words: BAC-FISH; microarray analysis; prenatal diagnosis; ring chromosome

How to Cite this Article:
Ohashi H, Suzumori K, Chisaka Y, Sonta S, Kobayashi T, Aoki Y, Matsubara Y, Sone M, Shaffer LG. 2011. Implications of prenatal diagnosis of the fetus with both interstitial deletion and a small marker ring originating from chromosome 5.
Am J Med Genet Part A 155:192–196.

INTRODUCTION

When genetic abnormalities are observed during prenatal screening, deletions, and supernumerary ring chromosomes are often seen separately [Gardner and Sutherland, 1996; Ryan et al., 1997; Slavotinek and Kingston, 1997]. Most cases with deletion of autosomes, even that of a tiny segment, are accompanied by clinical symptoms, including mental and developmental retardation; on the other hand, there have been examples of cases with deletion of autosomes without any abnormal features [Gardner and Sutherland, 1996; Daniel and Malafiej, 2003; Liehr et al., 2004].

Here, we describe a rare case with both interstitial deletion and a small ring originating from the same chromosome 5 detected prenatally and characterized by molecular cytogenetics. We emphasize the usefulness of molecular cytogenetics involving array-based comparative genomic hybridization (aCGH) and bacterial artificial chromosome (BAC)-fluorescent in situ hybridization BAC-FISH in providing precise information in cases of complex structural abnormality.

CLINICAL REPORT

Amniocentesis requested for advanced maternal age was performed in gestational week 16 on a 42-year-old woman with two

*Correspondence to:
Kaoru Suzumori, M.D., Ph.D., Fetal Life Science Center, 2-22-8 Chikusa, Chikusa-Ku, Nagoya 464-0858, Japan. E-mail: k.suzumori@flsc.jp
Published online 22 December 2010 in Wiley Online Library (wileyonlinelibrary.com).
DOI 10.1002/ajmg.a.33764

normal children. Fetal chromosomes were analyzed by GTG banding and multi-color fluorescent in situ hybridization (mFISH) using cultured amniocytes. After cytogenetic analyses, she was informed that one chromosome 5 with interstitial deletion and a small marker ring chromosome were detected in all the cells. Then, chromosomal analysis of the parents was performed on peripheral blood and showed normal karyotyes. It was difficult to offer additional molecular analyses within a limited term for pregnancy interruption. Ultrasonographic examination at 19 weeks of gestation did not detect any specific abnormality in the fetus. Despite possible unfavorable prognosis informed in genetic counseling, she and her spouse decided against termination of the pregnancy.

The pregnancy was uneventful and she delivered a phenotypically normal boy at 39 weeks of gestation. Apgar score was 8/8 and there were no particular clinical features. Body length, weight, and head circumference were within the normal range: 48 cm, 2,916 g, and 33 cm, respectively. After birth, we received informed consent to examine aCGH and BAC-FISH for further confirmation of the diagnosis.

Developmental, physical, and neurological examinations were normal and he appropriately reached his milestones. At 1 year and 6 months, his developmental quotient (DQ) was 110 (Fig. 1); echocardiography and brain imaging were also normal.

MOLECULAR CYTOGENETICSTUDIES

Chromosome and FISH Analyses

Cultured amniocytes were analyzed using G-banding with 540 bands per haploid number. G-banded chromosomes demonstrated that all cells had an interstitial deletion of chromosome 5 (5p11 → p13), and a small marker ring chromosome (Fig. 2A). The origin of this marker chromosome was unclear by G-banding. Therefore, the initial karyotyping was 47,XY,del(5)(p11p13), +mar. The mFISH revealed that the marker ring originated from chromosome 5, the same as the deleted chromosome (Fig. 2B). The ring chromosome seemed to have a centromere because this marker was detected in all cells. Chromosome analysis of the parents showed no abnormalities, indicating that these structural abnormalities in the fetus were de novo.

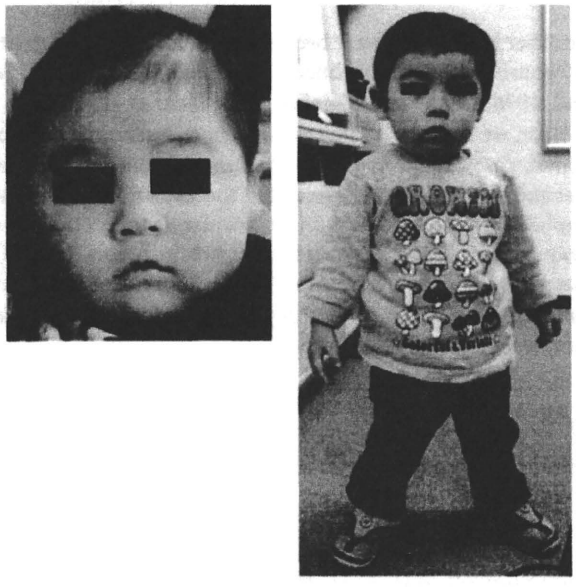

FIG. 1. Propositus at age 8 months (left picture) and 1 year 6 months (right picture). Note the phenotypically normal boy.

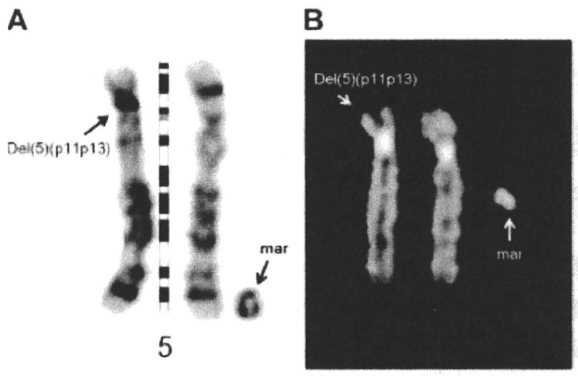

FIG. 2. Partial karyogram of chromosome 5, del(5p), and supernumerary ring by G-banding (A) and mFISH (B).

Oligonucelotide aCGH

For detection of gain and loss of chromosome segments, oligonucleotide-based microarray analysis was performed on reserved cultured amniocytes using a 105K-feature whole-genome microarray (Signature Chip Oligo Solution®, made for Signature Genomic Laboratories by Aligent Technologies Inc., Santa Clara, CA) [Ballif et al., 2008]. Microarray analysis of 1543 loci using on oligonucleotide array detected a complex abnormality in the DNA obtained from cultured amniocytes. Based on microarray analysis, this fetus had two duplications and a deletion of the short arm of chromosome 5. This abnormality was first characterized by a single copy gain of 380 oligonucleotide probes from the terminal end of the short arm of 5p, at 5p15.33p15.31. The extent of this duplication has been estimated to be approximately 6.1 Mb. The second alteration was characterized by a single copy loss of 347 oligonucleotide probes from 5p14.3p13.2. The extent of this interstitial deletion is estimated to be approximately 15.3 Mb. The third alteration was characterized by a single copy gain of 147 oligonucleotide probes from the pericentric region at 5p12p11. The extent of this duplication has been estimated to be approximately 3.4 Mb. Thus, this complex alteration resulted in partial trisomy 5p15.33–p15.31, partial monosomy 5p14.3–p13.2, and partial trisomy 5p12–p11. In conclusion, the result of microarray was arr5p15.33–p15.31(131,945–6,267,160)x3, 5p14.3–p13.2(21,438,495–36,736,934)x1, 5p12–p11(42,529,343–45,908,725)x3 (Fig. 3).

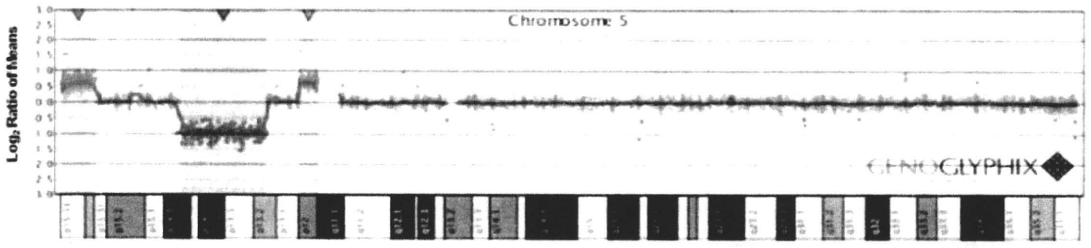

FIG. 3. Microarray plot showing, from left to right, a single copy gain of 380 oligonucleotide probes at 5p15.33p15.31, approximately 6.1 Mb in size; a single copy loss of 347 oligonucleotide probes from 5p14.3p13.2, approximately 15.3 Mb; and single copy gain of 147 oligonucleotide probes at 5p12p11, approximately 3.4 Mb in size. Probes are ordered on the x-axis according to physical mapping positions, with the distal p-arm on the left and the distal q-arm on the right.

BAC-FISH

For confirmation of the array results, FISH analyses were performed with BAC clones from duplicated and deleted regions as previously described [Shaffer et al., 1994; Traylor et al., 2009]. For this study, we used cord blood obtained at delivery.

FISH using a BAC clone from the 5p14.2 deleted region (RP11-701M20) and the 5p15.33 duplicated region (RP11-1006P13) identified an abnormal deleted (del) chromosome 5 that showed the loss of hybridization signals from the deleted region at 5p14.2 (Fig. 4A) and the presence of hybridization signals from the duplicated region at 5p15.33 (Fig. 4C). Interphase FISH

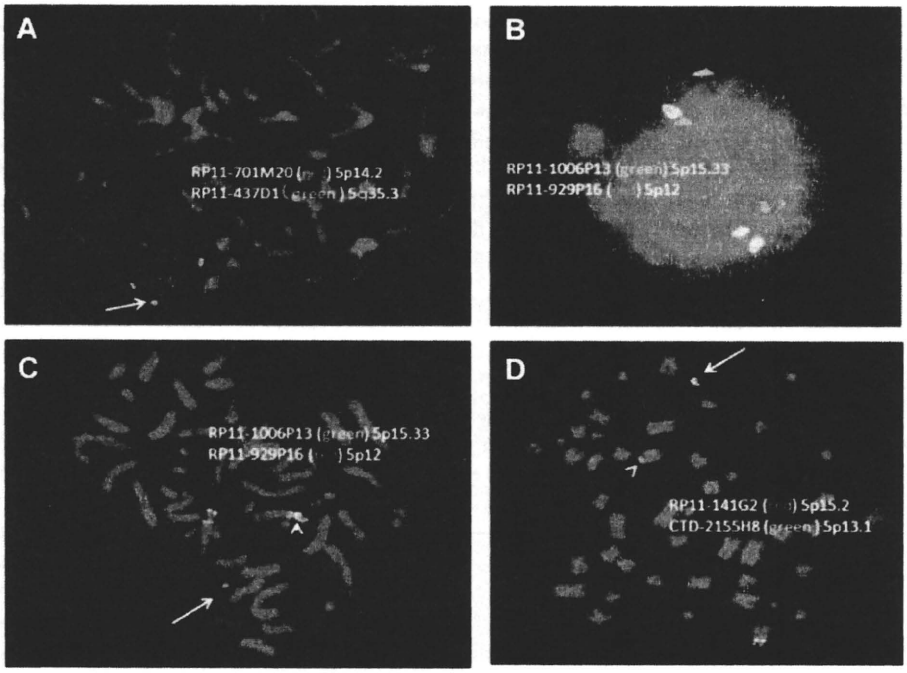

FIG. 4. FISH characterizations of a complex rearrangement on the short arm of chromosome 5. A: FISH showing a deletion of 5p14.2, BAC clone RP11-701M20 from 5p14.2 is labeled in red, and RP11-437D1 from 5q35.3 is labeled in green as a control. The presence of one red signal indicates deletion of 5p14.2 on one homologue (arrow). B,C: FISH with probes from the two regions is shown to be present in three copies by aCGH. BAC clone RP11-1006P13 from 5p15.33 is labeled in green, and RP11-929P16 from 5p12 is labeled in red. Interphase FISH (B) confirmed the presence of three copies of both regions. Metaphase FISH (C) shows a red signal but not a green signal on a small, supernumerary ring chromosome (arrow), indicating the presence of the 5p12 material on the supernumerary chromosome. Dotted green signals from 5p15.33 were present on the normal chromosome 5 homologs, but terminal duplicated signals were observed on one chromosome 5 (arrow head). D: FISH with probes from the intervening regions shown to be present in two copies by aCGH. BAC clone RP11-141G2 from 5p15.2 is labeled in red, and CTD-2155H8 from 5p13.1 is labeled in green. The supernumerary ring chromosome (arrow) shows a green signal and therefore the presence of material from 5p13.1, while one chromosome 5 homolog (arrowhead) shows a deletion for this region. The probe from 5p15.2 shows a normal hybridization pattern.

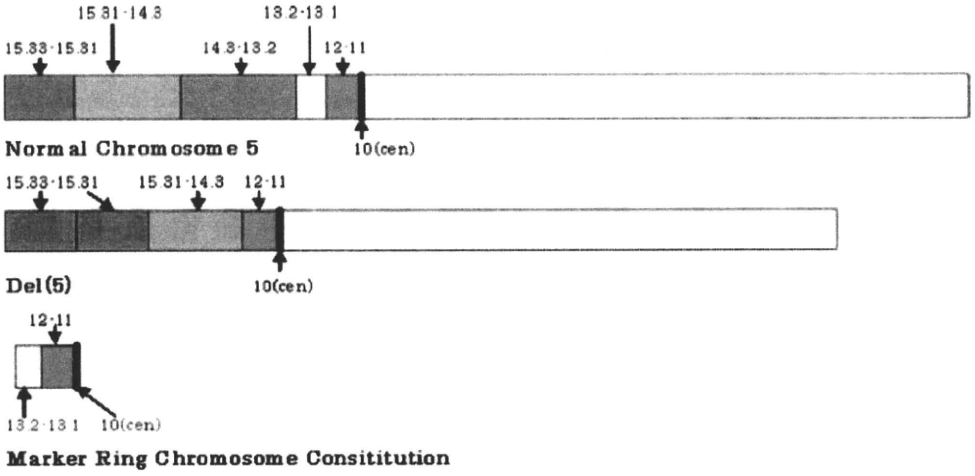

FIG. 5. Molecular background information on the deleted chromosome 5 and marker ring chromosome.

(Fig. 4B) clarified the presence of three copies of 5p15.33 and 5p12 regions. This del(5) also showed hybridization signals in an experiment using BAC clones from the first normal intervening sequence, between the terminal duplication and the deleted region, at 5p15.2 (RP11-141G2; Fig. 4D). Additional FISH analysis using a BAC clone from the 5p12 duplicated region (RP11-929P16) confirmed the origin of the marker ring chromosome (Fig. 4C). Hybridization signals from the second intervening normal sequence at 5p13.1 (CTD-2155H8), between the deleted region and the pericentric duplicated region, were also present on the marker ring chromosome, but not on the del(5), indicating that the deletion on that chromosome extends from 5p14.3 through 5p13.1 (Fig. 4D).

In conclusion, this baby had two abnormal derivative chromosomes. The first der(5) had an abnormal short arm with a duplication of 5p15.31 → 5p15.33, and a deletion of 5p13.1 → p14.3. The second der(5), the marker ring chromosome, was comprised of material from 5p10 → p13.2 (Fig. 5). The final karyotype of the baby is: 47,XY,ish der(5)(pter → p15.31::pter → p14.3::p11 → qter)(RP11-1006P13++,RP11-141G2+,RP11-701M20−,CTD-2155H8−),+der(5)(:13.2 → p10:)(CTD-2155H8+,RP11-929P16+).

DISCUSSION

Partial deletion of 5p is often seen in prenatal diagnoses and newborn analyses [Mainardi et al., 2001; Weiss et al., 2003]. In autosomes other than chromosome 5, deletions involving various chromosomes have also been reported in the literature [Gardner and Sutherland, 1996; Ryan et al., 1997; Slavotinek and Kingston, 1997]. Partial deletion of autosomes is generally accompanied by mild-to-severe clinical symptoms, including mental and developmental retardation in babies, although there have been exceptional cases where no clinical symptoms are observed [Callen et al., 1993; Overhauser et al., 1994; Knight et al., 1995]. Supernumerary marker chromosomes including small rings are also seen frequently in prenatal diagnoses [Michalski et al., 1993; Brøndum-Nielsen and Mikkelsen, 1995; Karaman et al., 2006]. Among babies with such small markers, some cases have no clinical features, but others showed mild-to-severe abnormalities after birth [Callen et al., 1993; Overhauser et al., 1994; Knight et al., 1995; Gardner and Sutherland, 1996; Daniel and Malafiej, 2003; Liehr et al., 2004; Bernardini et al., 2007]. Thus, in genetic counseling, it is important to offer chromosomal information from prenatal diagnoses and to provide as much detail as possible, including the origin and inheritance.

The present case had a deletion and a supernumerary marker ring chromosome. To our knowledge, this is the first report of detection by prenatal screening of both a deletion and a marker ring. In the literature, there are some mosaic cases of clones with a deletion and an additional ring separately [Gutiérrez-Angulo et al., 2002; Gereltzul et al., 2008; Kara et al., 2008], but such cases are extremely rare. In newborn infants, only one other case has been reported [Schuffenhauer et al., 1996] with a deletion and a ring of chromosome 5; this baby showed a mosaicism of 46,XY,del(5)/47,XY, del(5),+dic(5), with macrocephaly, asymmetric square skull, minor facial anomalies, omphalocele, inguinal hernias, hypospadias, and club feet. The break points of the deletion shared cen and p13 with those of the dicentric ring chromosome; this case had partial duplication of 5p (p13 → cen), and the mechanisms of del(5) and dic(5) were relatively straightforward. In the present case, on the other hand, the mechanisms of del(5) and marker ring [r(5)] were extremely complex. Microarray analysis revealed a terminal duplication, an interstitial deletion, and a pericentromeric duplication of the short arm of chromosome 5. Through this analysis, a total of six break points of the short arm of chromosome 5 (p15.33, p15.31, p14.3, p13.2, p12, and p11) were related to the formation of the structural abnormality with the duplication and the deletion, and the marker ring. According to the results of the G-band analysis of this case, we determined the break points of del(5) to be p11 and p13. However, assuming the microarray data are correct, the composition of r(5) becomes complicated, and explanation of the underlying mechanisms becomes difficult. To facilitate understanding of the exact composition of del(5) and r(5),

we performed FISH analysis using BAC clones from the duplicated 5p15.33, 5p12 regions and deleted 5p14.2 region. The short arm of the del(5) revealed a duplication of 5p15.31 → 5p15.33 and a deletion of 5p13.1 → p14.3. The r(5) was comprised of material from 5p10 → p13.2. Although supernumerary ring chromosome formation is difficult to determine, we speculate that this case have resulted from "centromere misdivision" along with a break in either the p or q arm, forming a small ring chromosome [Baldwin et al., 2008].

In summary, this complex 5p abnormality was characterized by a terminal duplication of 5p15.33p15.31 of approximately 6.4 Mb, an interstitial deletion 15p14.3p13.2 of approximately 15.3 Mb and an interstitial duplication of 5p12p11 of approximately 3.4 Mb. The 5p terminal duplication contained at least 21 genes including ADAMTS16, AHRR, and C5orf38. The 5p14.3p13.2 deletion lacked at least 22 genes including *CDH12*, *PRDM9*, *CDH10*, and *DH9*. The 5p12p11 duplication contained at least 11 genes including *GHR*, *SEPP1*, *C5orf39*, and *ZNF11131*.

When the child was examined at 1 year and 6 months, we could not find any developmental abnormality, either physical or mental. Because of his age he will need to be followed to confirm normal intellectual development. In order to provide accurate and useful genetic counseling in similar cases in the future, the accumulation of further reports with complicated chromosome abnormalities would be beneficial.

REFERENCES

Baldwin EL, May LE, Justice AN, Martin CL, Ledbetter DH. 2008. Mechanism and consequences of small supernumerary marker chromosomes: From Barbara McClintock to modern genetic-counseling issue. Am J Hum Genet 82:398–410.

Ballif BC, Theisen A, McDonald-McGinn DM, Zackai EH, Bejjanni BA, Shaffer LG. 2008. Identification of a previously unrecognized microdeletion syndrome of 16q11.2q12.2. Clin Genet 74:469–475.

Bernardini L, Capalbo A, D'Avanzo MG, Torrente I, Grammatico P, Dell'Edera D, Cavalcanti DP, Novelli A, Dallapiccola B. 2007. Five cases of supernumerary small ring chromosomes 1: Heterogeneity and genotype–phenotype correlation. Eur J Med Genet 50:94–102.

Brøndum-Nielsen K, Mikkelsen M. 1995. A 10-year survey, 1980–1990, of prenatally diagnosed small supernumerary marker chromosomes, identified by FISH analysis. Outcome and follow-up of 14 cases diagnosed in a series of 12,699 prenatal samples. Prenat Diagn 15:615–619.

Callen DF, Eyre H, Lane S, Shen Y, Hansmann I, Spinner N, Zackai E, McDonald-McGinn D, Schuffenhauer S, Wauters J, Van Thienen M-N, Van Roy B, Sutherland GR, Haan EA. 1993. High resolution mapping of interstitial long arm deletions of chromosome 16: Relationship to phenotype. J Med Genet 30:828–832.

Daniel A, Malafiej P. 2003. A series of supernumerary small ring marker autosomes identified by FISH with chromosome probe arrays and literature review excluding chromosome 15. Am J Med Genet Part A 117A:212–222.

Gardner RJM, Sutherland GR. 1996. Chromosome Abnormalities and Genetic Counseling. 2nd edition. New York, Oxford: Oxford University Press. pp. 1–478.

Gereltzul E, Baba Y, Suda N, Shiga M, Inoue MS, Tsuji M, Shin I, Hirata Y, Ohyama K, Moriyama K. 2008. Case report of de novo dup(18p)/del-(18q) and r(18) mosaicism. J Hum Genet 53:941–946.

Gutiérrez-Angulo M, Lazalde B, Vasquez AI, Leal C, Corral E, Rivera H. 2002. del(X)(p22.1)/r(X)(p22.1q28) Dynamic mosaicism in a Turner syndrome patient. Ann Genet 45:17–20.

Kara N, Okten G, Gunes SO, Saglam Y, Tasdemir HA, Pinarli FA. 2008. An epileptic case with mosaic ring chromosome 6 and 6q terminal deletion. Epilepsy Res 80:219–223.

Karaman B, Aytan M, Yilmaz K, Toksoy G, Onal EP, Ghanbari A, Engur A, Kayserili H, Yuksel-Apak M, Basaran S. 2006. The identification of small supernumerary marker chromosomes; the experiences of 15,792 fetal karyotyping from Turkey. Eur J Med Genet 49:207–214.

Knight LA, Yong MH, Tan M, Ng IS. 1995. Del(3) (p25.3) without phenotypic effect. J Med Genet 32:994–995.

Liehr T, Claussen U, Starke H. 2004. Small supernumerary marker chromosomes (sSMC) in humans. Cytogenet Genome Res 107:55–67.

Mainardi PC, Perfumo C, Calì A, Coucourde G, Pastore G, Cavani S, Zara F, Overhauser J, Pierluigi M, Bricarelli FD. 2001. Clinical and molecular characterization of 80 patients with 5p deletion: Genotype–phenotype correlation. J Med Genet 38:151–158.

Michalski K, Rauer M, Williamson N, Perszyk A, Hoo JJ. 1993. Identification, counselling, and outcome of two cases of prenatally diagnosed supernumerary small ring chromosomes. Am J Med Genet 46:88–94.

Overhauser J, Huang X, Gersh M, Wilson W, McMahon J, Bengtsson U, Rojas K, Meyer M, Wasmuth JJ. 1994. Molecular and phenotypic mapping of the short arm of chromosome 5: Sublocalization of the critical region for the cri-du-chat syndrome. Hum Mol Genet 3:247–252.

Ryan AK, Goodship JA, Wilson DI, Philip N, Levy A, Seidel H, Schuffenhauer S, Oechsler H, Belohradsky B, Prieur M, Aurias A, Raymond FL, Clayton-Smith J, Hatchwell E, McKeown C, Beemer FA, Dallapiccola B, Novelli G, Hurst JA, Ignatius J, Green AJ, Winter RM, Brueton L, Brøndum-Nielsen K, Stewart F, Van Essen T, Patton M, Paterson J, Scambler PJ. 1997. Spectrum of clinical features associated with interstitial chromosome 22q11 deletions: A European collaborative study. J Med Genet 34:798–804.

Schuffenhauer S, Kobelt A, Daumer-Haas C, Löffler C, Müller G, Murken J, Meitinger T. 1996. Interstitial deletion 5p accompanied by dicentric ring formation of the deleted segment resulting in trisomy 5p13-cen. Am J Med Genet 65:56–59.

Shaffer LG, McCaskill C, Han J-Y, Choo KHA, Cutillo DM, Donnenfeld AE, Weiss L, Van Dyke DL. 1994. Molecular characterization of de novo secondary trisomy 13. Am J Hum Genet 55:968–974.

Slavotinek A, Kingston H. 1997. Interstitial deletion of bands 4q12 → q13.1: Case report and review of proximal 4q deletions. J Med Genet 34:862–865.

Traylor R, Fan Z, Ballif BC. 2009. Micordeletion of 6q16.1 encompassing EPHA7 in a child with mild neurological abnormalities and dysmorphic features: Case report. Mol Cytogenet 2:1–6.

Weiss A, Shalev S, Weiner E, Shneor Y, Shalev E. 2003. Prenatal diagnosis of 5p deletion syndrome following abnormally low maternal serum human chorionic gonadotrophin. Prenat Diagn 23:572–574.

Journal of Human Genetics (2011) 56, 91–93

www.nature.com/jhg

SHORT COMMUNICATION

Androgenetic/biparental mosaicism in a girl with Beckwith–Wiedemann syndrome-like and upd(14)pat-like phenotypes

Kazuki Yamazawa[1,5], Kazuhiko Nakabayashi[2], Kentaro Matsuoka[3], Keiko Masubara[1], Kenichiro Hata[2], Reiko Horikawa[4] and Tsutomu Ogata[1]

This report describes androgenetic/biparental mosaicism in a 4-year-old Japanese girl with Beckwith–Wiedemann syndrome (BWS)-like and paternal uniparental disomy 14 (upd(14)pat)-like phenotypes. We performed methylation analysis for 18 differentially methylated regions on various chromosomes, genome-wide microsatellite analysis for a total of 90 loci and expression analysis of *SNRPN* in leukocytes. Consequently, she was found to have an androgenetic 46,XX cell lineage and a normal 46,XX cell lineage, with the frequency of the androgenetic cells being roughly calculated as 91% in leukocytes, 70% in tongue tissues and 79% in tonsil tissues. It is likely that, after a normal fertilization between an ovum and a sperm, the paternally derived pronucleus alone, but not the maternally derived pronucleus, underwent a mitotic division, resulting both in the generation of the androgenetic cell lineage by endoreplication of one blastomere containing a paternally derived pronucleus and in the formation of the normal cell lineage by union of paternally and maternally derived pronuclei. It appears that the extent of overall (epi)genetic aberrations exceeded the threshold level for the development of BWS-like and upd(14)pat-like phenotypes, but not for the occurrence of other imprinting disorders or recessive Mendelian disorders.
Journal of Human Genetics (2011) **56,** 91–93; doi:10.1038/jhg.2010.142; published online 11 November 2010

Keywords: androgenesis; Beckwith–Wiedemann syndrome; mosaicism; upd(14)pat

INTRODUCTION

A pure androgenetic human with paternal uniparental disomy for all chromosomes is incompatible with life because of genomic imprinting.[1,2] However, a human with an androgenetic cell lineage could be viable in the presence of a normal cell lineage. Indeed, an androgenetic cell lineage has been identified in six liveborn individuals with variable phenotypes.[3–7] All the androgenetic cell lineages have a 46,XX karyotype, and this is consistent with the lethality of an androgenetic 46,YY cell lineage.

Here, we report on a girl with androgenetic/biparental mosaicism, and discuss the underlying factors for the phenotypic development.

CASE REPORT

This patient was conceived naturally to non-consanguineous and healthy parents. At 24 weeks gestation, the mother was referred to us because of threatened premature delivery. Ultrasound studies showed Beckwith–Wiedemann syndrome (BWS)-like features,[8] such as macroglossia, organomegaly and umbilical hernia, together with polyhydramnios and placentomegaly. The mother repeatedly received amnioreduction and tocolysis.

She was delivered by an emergency cesarean section because of preterm rupture of membranes at 34 weeks of gestation. Her birth weight was 3730 g (+4.8 s.d. for gestational age), and her length 45.6 cm (+0.7 s.d.). The placenta weighed 1040 g (+7.3 s.d.).[9] She was admitted to a neonatal intensive care unit due to asphyxia. Physical examination confirmed a BWS-like phenotype. Notably, chest roentgenograms delineated mild bell-shaped thorax characteristic of paternal uniparental disomy 14 (upd(14)pat),[10] although coat hanger appearance of the ribs indicative of upd(14)pat was absent (Supplementary Figure 1). She was placed on mechanical ventilation for 2 months, and received tracheostomy, glossectomy and tonsillectomy in her infancy, due to upper airway obstruction. She also had several clinical features occasionally reported in BWS[8] (Supplementary Table 1). Her karyotype was 46,XX in all the 50 lymphocytes analyzed. On the last examination at 4 years of age, she showed postnatal growth failure and severe developmental retardation.

[1]Department of Molecular Endocrinology, National Research Institute for Child Health and Development, Tokyo, Japan; [2]Department of Maternal-Fetal Biology, National Research Institute for Child Health and Development, Tokyo, Japan; [3]Division of Pathology, National Medical Center for Children and Mothers, Tokyo, Japan and [4]Division of Endocrinology and Metabolism, National Medical Center for Children and Mothers, Tokyo, Japan
[5]Current address: Department of Physiology, Development & Neuroscience, University of Cambridge, Cambridge, UK.
Correspondence: Dr T Ogata, Department of Molecular Endocrinology, National Research Institute for Child Health and Development, 2-10-1 Ohkura, Setagaya, Tokyo 157-8535, Japan.
E-mail: tomogata@nch.go.jp
Received 9 September 2010; revised 18 October 2010; accepted 22 October 2010; published online 11 November 2010

MOLECULAR STUDIES

This study was approved by the Institutional Review Board Committee at the National Center for Child health and Development, and performed after obtaining informed consent.

Methylation analysis

We first performed bisulfite sequencing for the *H19*-DMR (differentially methylated region) and KvDMR1 as a screening of BWS[11,12] and that for the IG-DMR and the *MEG3*-DMR as a screening of upd(14)pat,[10] using leukocyte genomic DNA. Paternally derived clones were predominantly identified for the four DMRs examined (Figure 1a). We next performed combined bisulfite restriction analysis for multiple DMRs, as reported previously.[13] All the autosomal DMRs exhibited markedly skewed methylation patterns consistent with predominance of paternally inherited clones, whereas the *XIST*-DMR on the X chromosome showed a normal methylation pattern (Figure 1a).

Genome-wide microsatellite analysis

Microsatellite analysis was performed for 90 loci with high heterozygosities in the Japanese population.[14] Major peaks consistent with paternal uniparental isodisomy and minor peaks of maternal origin were identified for at least one locus on each chromosome, with the minor peaks of maternal origin being more obvious in tongue and tonsil tissues than in leukocytes (Figure 1b and Supplementary Table 2). There were no loci with three or four peaks indicative of chimerism. The frequency of the androgenetic cells was calculated as 91% in leukocytes, 70% in tongue cells and 79% in tonsil cells, although the estimation apparently was a rough one (for details, see Supplementary Methods).

Expression analysis

We examined *SNRPN* expression, because *SNRPN* showed strong expression in leukocytes (for details, see Supplementary Data). *SNRPN* expression was almost doubled in the leukocytes of this patient (Figure 1c).

DISCUSSION

These results suggest that this patient had an androgenetic 46,XX cell lineage and a normal 46,XX cell lineage. In this regard, both the androgenetic and the biparental cell lineages appear to have derived from a single sperm and a single ovum, because a single haploid genome of paternal origin and that of maternal origin were identified in this patient by genome-wide microsatellite analysis. Thus, it is likely that after a normal fertilization between an ovum and a sperm, the paternally derived pronucleus alone, but not the maternally derived pronucleus, underwent a mitotic division, resulting both in the generation of the androgenetic cell lineage by endoreplication of

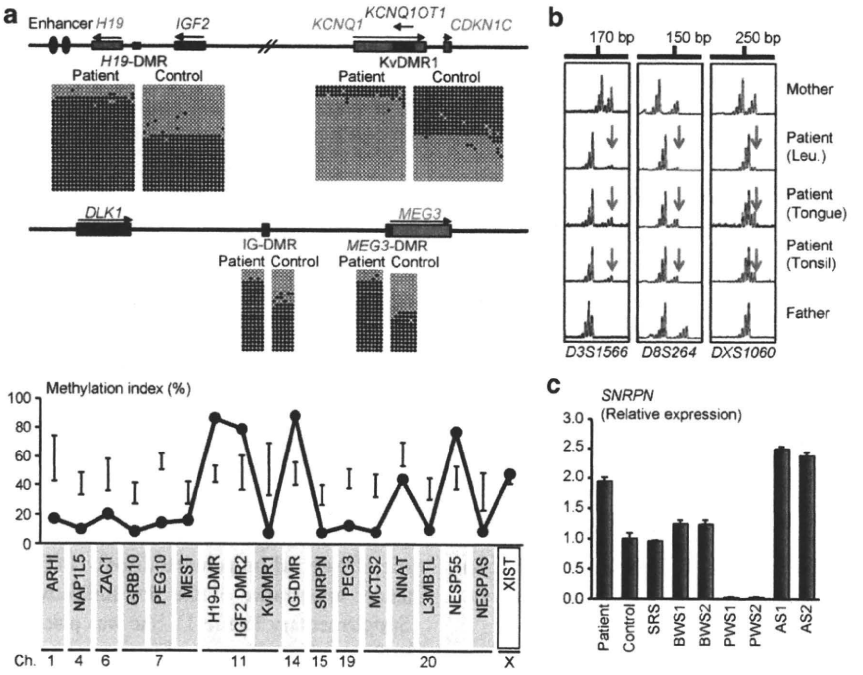

Figure 1 Representative molecular results. (**a**) Methylation analysis. Upper part: Bisulfite sequencing data for the *H19*-DMR and the KvDMR1 on 11p15.5, and those for the IG-DMR and the *MEG3*-DMR on 14q32.2. Each line indicates a single clone, and each circle denotes a CpG dinucleotide; filled and open circles represent methylated and unmethylated cytosines, respectively. Paternally expressed genes are shown in blue, maternally expressed gene in red, and the DMRs in green. The *H19*-DMR, the IG-DMR, and the *MEG3*-DMR are usually methylated after paternal transmission and unmethylated after maternal transmission, whereas the KvDMR1 is usually unmethylated after paternal transmission and methylated after maternal transmission.[10,11] Lower part: Methylation indices (the ratios of methylated clones) obtained from the COBRA analyses for the 18 DMRs. The DMRs highlighted in blue and pink are methylated after paternal and maternal transmissions, respectively. The black vertical bars indicate the reference data (maximum – minimum) in leukocyte genomic DNA of 20 normal control subjects (the *XIST*-DMR data are obtained from 16 control females). (**b**) Representative microsatellite analysis. Major peaks of paternal origin and minor peaks of maternal origin (red arrows) have been identified in this patient. The minor peaks of maternal origin are more obvious in tongue and tonsil tissues than in leukocytes (Leu.). (**c**) Relative expression level (mean ± s.d.) of *SNRPN*. The data are normalized against *TBP*. SRS: an SRS patient with an epimutation (hypomethylation) of the *H19*-DMR; BWS1: a BWS patient with an epimutation (hypermethylation) of the *H19*-DMR; BWS2: a BWS patient with upd(11)pat; PWS1: a Prader-Willi syndrome (PWS) patient with upd(15)mat; PWS2: a PWS patient with an epimutation (hypermethylation) of the *SNRPN*-DMR; AS1: an Angelman syndrome (AS) patient with upd(15)pat; and AS2: an AS patient with an epimutation (hypomethylation) of the *SNRPN*-DMR. The data were obtained using an ABI Prism 7000 Sequence Detection System (Applied Biosystems).

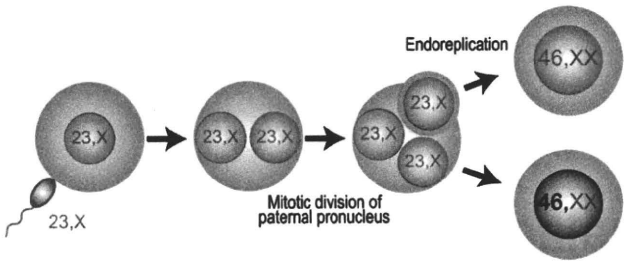

Figure 2 Schematic representation of the generation of the androgenetic/biparental mosaicism. Polar bodies are not shown.

one blastomere containing a paternally derived pronucleus and in the formation of the normal cell lineage by union of paternally and maternally derived pronuclei (Figure 2). This model has been proposed for androgenetic/biparental mosaicism generated after fertilization between a single ovum and a single sperm.[5,15,16] The normal methylation pattern of the *XIST*-DMR is explained by assuming that the two X chromosomes in the androgenetic cell lineage undergo random X-inactivation, as in the normal cell lineage. Furthermore, the results of microsatellite analysis imply that the androgenetic cells were more prevalent in leukocytes than in tongue and tonsil tissues.

A somatic androgenetic cell lineage has been identified in seven liveborn patients including this patient (Supplementary Table 1).[3–7] In this context, leukocytes are preferentially utilized for genetic analyses in human patients, and detailed examinations such as analyses of plural DMRs are necessary to detect an androgenetic cell lineage. Thus, the hitherto identified patients would be limited to those who had androgenetic cells as a predominant cell lineage in leukocytes probably because of a stochastic event and received detailed molecular studies. If so, an androgenetic cell lineage may not be so rare, and could be revealed by detailed analyses as well as examinations of additional tissues in patients with relatively complex phenotypes, as observed in the present patient.

Phenotypic features in androgenetic/biparental mosaicism would be determined by several factors. They include (1) the ratio of two cell lineages in various tissues/organs, (2) the number of imprinted domains relevant to specific features (for example, dysregulation of the imprinted domains on 11p15.5 and 14q32.2 is involved in placentomegaly[9,17]), (3) the degree of clinical effects of dysregulated imprinted domains (an (epi)dominant effect has been assumed for the 11p15.5 imprinted domains[18]), (4) expression levels of imprinted genes in androgenetic cells (although *SNRPN* expression of this patient was consistent with androgenetic cells being predominant in leukocytes, complicated expression patterns have been identified for several imprinted genes in both androgenetic and parthenogenetic fetal mice, probably because of perturbed *cis*- and *trans*-acting regulatory mechanisms[19]) and (5) unmasking of possible paternally inherited recessive mutation(s) in androgenetic cells. Thus, in this patient, it appears that the extent of overall (epi)genetic aberrations exceeded the threshold level for the development of BWS-like and upd(14)pat-like body and placental phenotypes, but remained below the threshold level for the occurrence of other imprinting disorders or recessive Mendelian disorders.

CONFLICT OF INTEREST

The authors declare no conflict of interest.

ACKNOWLEDGEMENTS

This work was supported by grants from the Ministry of Health, Labor, and Welfare, and the Ministry of Education, Science, Sports and Culture.

1 Surani, M. A., Barton, S. C. & Norris, M. L. Development of reconstituted mouse eggs suggests imprinting of the genome during gametogenesis. *Nature* **308,** 548–550 (1984).
2 McGrath, J. & Solter, D. Completion of mouse embryogenesis requires both the maternal and paternal genomes. *Cell* **37,** 179–183 (1984).
3 Hoban, P. R., Heighway, J., White, G. R., Baker, B., Gardner, J., Birch, J. M. *et al.* Genome-wide loss of maternal alleles in a nephrogenic rest and Wilms' tumour from a BWS patient. *Hum. Genet.* **95,** 651–656 (1995).
4 Bryke, C. R., Garber, A. T. & Israel, J. Evolution of a complex phenotype in a unique patient with a paternal uniparental disomy for every chromosome cell line and a normal biparental inheritance cell line. *Am. J. Hum. Genet.* **75**(Suppl), 831 (2004).
5 Giurgea, I., Sanlaville, D., Fournet, J. C., Sempoux, C., Bellanne-Chantelot, C. & Touati, G. Congenital hyperinsulinism and mosaic abnormalities of the ploidy. *J. Med. Genet.* **43,** 248–254 (2006).
6 Wilson, M., Peters, G., Bennetts, B., McGillivray, G., Wu, Z. H., Poon, C. *et al.* The clinical phenotype of mosaicism for genome-wide paternal uniparental disomy: two new reports. *Am. J. Med. Genet. Part A* **146A,** 137–148 (2008).
7 Reed, R. C., Beischel, L., Schoof, J., Johnson, J., Raff, M. L. & Kapur, R. P. Androgenetic/biparental mosaicism in an infant with hepatic mesenchymal hamartoma and placental mesenchymal dysplasia. *Pediatr. Dev. Pathol.* **11,** 377–383 (2008).
8 Jones, K. L. *Smith's Recognizable Patterns of Human Malformation* 6th edn. (Elsevier Saunders: Philadelphia, 2006).
9 Kagami, M., Yamazawa, K., Matsubara, K., Matsuo, N. & Ogata, T. Placentomegaly in paternal uniparental disomy for human chromosome 14. *Placenta* **29,** 760–761 (2008).
10 Kagami, M., Sekita, Y., Nishimura, G., Irie, M., Kato, F., Okada, M. *et al.* Deletions and epimutations affecting the human 14q32.2 imprinted region in individuals with paternal and maternal upd(14)-like phenotypes. *Nat. Genet.* **40,** 237–242 (2008).
11 Yamazawa, K., Kagami, M., Nagai, T., Kondoh, T., Onigata, K., Maeyama, K. *et al.* Molecular and clinical findings and their correlations in Silver-Russell syndrome: implications for a positive role of IGF2 in growth determination and differential imprinting regulation of the IGF2-H19 domain in bodies and placentas. *J. Mol. Med.* **86,** 1171–1181 (2008).
12 Weksberg, R., Shuman, C. & Beckwith, J. B. Beckwith-Wiedemann syndrome. *Eur. J. Hum. Genet.* **18,** 8–14 (2010).
13 Yamazawa, K., Nakabayashi, K., Kagami, M., Sato, T., Saitoh, S., Horikawa, R. *et al.* Parthenogenetic chimaerism/mosaicism with a Silver-Russell syndrome-like phenotype. *J. Med. Genet.* **47,** 782–785 (2010).
14 Ikari, K., Onda, H., Furushima, K., Maeda, S., Harata, S. & Takeda, J. Establishment of an optimized set of 406 microsatellite markers covering the whole genome for the Japanese population. *J. Hum. Genet.* **46,** 207–210 (2001).
15 Kaiser-Rogers, K. A., McFadden, D. E., Livasy, C. A., Dansereau, J., Jiang, R., Knops, J. F. *et al.* Androgenetic/biparental mosaicism causes placental mesenchymal dysplasia. *J. Med. Genet.* **43,** 187–192 (2006).
16 Kotzot, D. Complex and segmental uniparental disomy updated. *J. Med. Genet.* **45,** 545–556 (2008).
17 Monk, D., Arnaud, P., Apostolidou, S., Hills, F. A., Kelsey, G., Stanier, P. *et al.* Limited evolutionary conservation of imprinting in the human placenta. *Proc. Natl. Acad. Sci. USA.* **103,** 6623–6628 (2006).
18 Azzi, S., Rossignol, S., Steunou, V., Sas, T., Thibaud, N., Danton, F. *et al.* Multilocus methylation analysis in a large cohort of 11p15-related foetal growth disorders (Russell Silver and Beckwith Wiedemann syndromes) reveals simultaneous loss of methylation at paternal and maternal imprinted loci. *Hum. Mol. Genet.* **18,** 4724–4733 (2009).
19 Ogawa, H., Wu, Q., Komiyama, J., Obata, Y. & Kono, T. Disruption of parental-specific expression of imprinted genes in uniparental fetuses. *FEBS Lett.* **580,** 5377–5384 (2006).

Supplementary Information accompanies the paper on Journal of Human Genetics website (http://www.nature.com/jhg)

Heterozygous Orthodenticle Homeobox 2 Mutations Are Associated with Variable Pituitary Phenotype

Sumito Dateki, Kitaro Kosaka, Kosei Hasegawa, Hiroyuki Tanaka, Noriyuki Azuma, Susumu Yokoya, Koji Muroya, Masanori Adachi, Toshihiro Tajima, Katsuaki Motomura, Eiichi Kinoshita, Hiroyuki Moriuchi, Naoko Sato, Maki Fukami, and Tsutomu Ogata

Department of Endocrinology and Metabolism (S.D., N.S., M.F., T.O.), National Research Institute for Child Health and Development, and Division of Ophthalmology (N.A.) and Department of Medical Subspecialties (S.Y.), National Children's Medical Center, Tokyo 157-8535, Japan; Department of Pediatrics (S.D., K.M., E.K., H.M.), Nagasaki University Graduate School of Biomedical Sciences, Nagasaki 852-8501, Japan; Department of Pediatrics (K.K.), Kyoto Prefectural University of Medicine, Graduate School of Medical Science, Kyoto 602-8566, Japan; Department of Pediatrics (K.H., H.T.), Okayama University Graduate School of Medicine, Dentistry, and Pharmaceutical Sciences, Okayama 700-8558, Japan; Division of Endocrinology and Metabolism (K.M., M.A.), Kanagawa Children's Medical Center, Yokohama 232-8555, Japan; and Department of Pediatrics (T.T.), Hokkaido University School of Medicine, Sapporo 060-8638, Japan

Context: Although recent studies have suggested a positive role of *OTX2* in pituitary as well as ocular development and function, detailed pituitary phenotypes in *OTX2* mutations and *OTX2* target genes for pituitary function other than *HESX1* and *POU1F1* remain to be determined.

Objective: We aimed to examine such unresolved issues.

Subjects: We studied 94 Japanese patients with various ocular or pituitary abnormalities.

Results: We identified heterozygous p.K74fsX103 in case 1, p.A72fsX86 in case 2, p.G188X in two unrelated cases (3 and 4), and a 2,860,561-bp microdeletion involving *OTX2* in case 5. Clinical studies revealed isolated GH deficiency in cases 1 and 5; combined pituitary hormone deficiency in case 3; abnormal pituitary structures in cases 1, 3, and 5; and apparently normal pituitary function in cases 2 and 4, together with ocular anomalies in cases 1–5. The wild-type Orthodenticle homeobox 2 (OTX2) protein transactivated the *GNRH1* promoter as well as the *HESX1*, *POU1F1*, and *IRBP* (interstitial retinoid-binding protein) promoters, whereas the p.K74fsX103-OTX2 and p.A72fsX86-OTX2 proteins had no transactivation functions and the p.G188X-OTX2 protein had reduced (~50%) transactivation functions for the four promoters, with no dominant-negative effect. cDNA screening identified positive *OTX2* expression in the hypothalamus.

Conclusions: The results imply that *OTX2* mutations are associated with variable pituitary phenotype, with no genotype-phenotype correlations, and that *OTX2* can transactivate *GNRH1* as well as *HESX1* and *POU1F1*. **(*J Clin Endocrinol Metab* 95: 756–764, 2010)**

Pituitary development and function depends on the spatially and temporally controlled expression of multiple transcription factor genes such as *POU1F1*, *HESX1*, *LHX3*, *LHX4*, *PROP1*, and *SOX3* (1, 2). Whereas mutations of some genes (*e.g. POU1F1*) result in a relatively characteristic pattern of pituitary hormone deficiency, those of other genes (*e.g. HESX1*) are associated with a wide range of pituitary phenotype including combined pi-

ISSN Print 0021-972X ISSN Online 1945-7197
Printed in U.S.A.

doi: 10.1210/jc.2009-1334 Received June 23, 2009. Accepted November 9, 2009.
First Published Online December 4, 2009

Abbreviations: CGH, Comparative genomic hybridization; CPHD, combined pituitary hormone deficiency; EPP, ectopic posterior pituitary; FISH, fluorescence *in situ* hybridization; HD, homeodomain; IGHD, isolated GH deficiency; IRBP, interstitial retinoid-binding protein; MLPA, multiplex ligation-dependent probe amplification; NMD, nonsense mediated mRNA decay; OTX2, orthodenticle homeobox 2; PH, pituitary hypoplasia; SOD, septooptic dysplasia; TD, transactivation domain.

tuitary hormone deficiency (CPHD), isolated GH deficiency (IGHD), and apparently normal phenotype. However, because mutations of these genes account for a relatively minor portion of patients with congenital hypopituitarism (2, 3), multiple genes would remain to be identified in congenital hypopituitarism.

Orthodenticle homeobox 2 (*OTX2*) is a transcription factor gene primarily involved in ocular development (4). It encodes a paired type homeodomain (HD) and a transactivation domain (TD) and produces two functionally similar splice variants, isoform-a (GenBank accession no. NM_21728.2) and isoform-b (NM_172337.1) with and without eight amino acids because of alternative splice acceptor sites at the boundary of intron 3 and exon 4 (5). To date, at least 10 pathological heterozygous *OTX2* mutations have been identified in patients with ocular malformations such as anophthalmia and/or microphthalmia (6, 7). Ocular phenotype is highly variable, ranging from anophthalmia to nearly normal eye development, even in patients from the same family. Furthermore, most patients also exhibit brain anomaly, seizure, and/or developmental delay.

Recent studies have indicated that *OTX2* is also involved in pituitary development and function. Dateki *et al.* (8) showed that *OTX2* is expressed in the pituitary and has a transactivation function for the promoters of *POU1F1* and *HESX1* as well as the promoter of *IRBP* (interstitial retinoid-binding protein) involved in ocular function and that a frameshift *OTX2* mutation identified in a patient with bilateral anophthalmia and partial IGHD barely retained the transactivation activities. Subsequently a missense *OTX2* mutation with a dominant-negative effect and a frameshift *OTX2* mutation with loss-of-function effect were identified in CPHD patients with and without ocular malformation (9, 10).

However, detailed pituitary phenotypes in *OTX2* mutation-positive patients as well as other possible *OTX2* target genes for pituitary development and function remain to be determined. Here we report five new patients with *OTX2* mutations and summarize clinical findings in *OTX2* mutation-positive patients. We also show that *OTX2* is expressed in the hypothalamus and has a transactivation function for the promoter of *GNRH1*.

Patients and Methods

Patients

We studied 94 Japanese patients consisting of: 1) 16 patients with ocular anomalies and pituitary dysfunctions accompanied by short stature (< −2 SD) (six with anophthalmia and/or microphthalmia and CPHD, five with anophthalmia and/or microphthalmia and IGHD, three with septooptic dysplasia (SOD) and CPHD, and two with SOD and IGHD) (group 1); 2) 12 patients with ocular anomalies whose pituitary functions were not investigated (one with bilateral microphthalmia and short stature, one with bilateral optic nerve hypoplasia and short stature, and 10 with anophthalmia and/or microphthalmia and normal stature) (group 2); and 3) 66 patients with pituitary dysfunctions but without ocular anomalies (five with IGHD and 61 patients with CPHD) (group 3). No demonstrable mutation was identified for *HESX1* in patients with SOD, *GH1* and *HESX1* in patients with IGHD, and *POU1F*, *HESX1*, *LHX3*, *LHX4*, *PROP1*, and *SOX3* in patients with various types of CPHD (2). All the patients had normal karyotype.

Primers and probes

The primers and probes used in this study are shown in Supplemental Table 1, published as supplemental data on The Endocrine Society's Journals Online web site at http://jcem.endojournals.org.

Sequence analysis of OTX2

This study was approved by the Institutional Review Board Committee at National Center for Child Health and Development. After obtaining written informed consent, the coding exons 3-5 and their flanking splice sites were PCR amplified using leukocyte genomic DNA samples of all 94 patients and were subjected to direct sequencing on a CEQ 8000 autosequencer (Beckman Coulter, Fullerton, CA). To confirm a heterozygous mutation, the corresponding PCR products were subcloned with TOPO TA cloning kit (Invitrogen, Carlsbad, CA), and normal and mutant alleles were sequenced separately.

Prediction of the occurrence of aberrant splicing and nonsense mediated mRNA decay (NMD)

To examine whether identified mutations could cause aberrant splicing by creating or disrupting exonic splicing enhancers and/or splice sites (11, 12), we performed *in silico* analyses with the ESE finder release 3.0 (http://rulai.cshl.edu/cgi-bin/tools/ESE3/esefinder.cgi) for the prediction of exonic splice enhancers and with the program at the Berkeley Drosophila Genome Project (http://www.fruitfly.org/seq_tools/splice.html) for the prediction of splice sites. We also analyzed whether identified mutations could be subject to NMD on the basis of the previous report (12, 13).

Deletion analysis

Multiplex ligation-dependent probe amplification (MLPA) was performed for *OTX2* intragenic mutation-negative patients as a screening of a possible microdeletion affecting *OTX2*. This procedure was performed according to the manufacturer's instructions (14), using probes designed specifically for *OTX2* exon 4 together with a commercially available MLPA probe mix (P236) (MRC-Holland, Amsterdam, The Netherlands) used as internal controls. To confirm a microdeletion, fluorescence *in situ* hybridization (FISH) was performed with a long PCR product for *OTX2* (a 6096 bp segment from intron 2 to exon 5) together with an RP11-566I2 BAC probe (14q11.2; Invitrogen, Carlsbad, CA) used as an internal control. The probe for *OTX2* was labeled with digoxigenin and detected by rhodamine anti-digoxigenin, and the control probe was labeled with biotin and

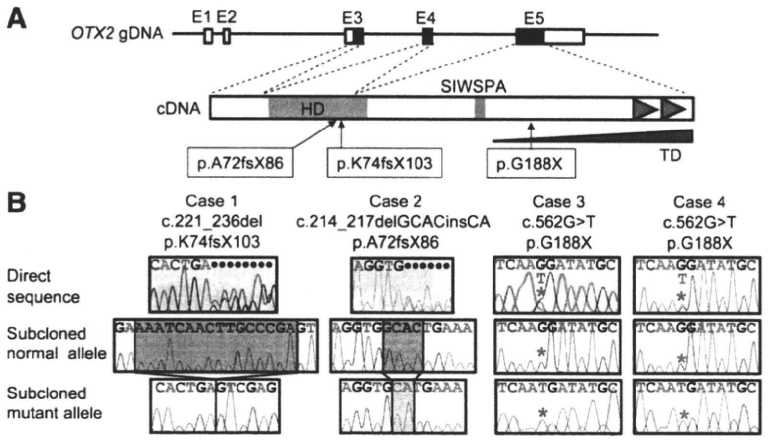

FIG. 1. Sequence analysis in cases 1–4. A, The structure of *OTX2* (the isoform-b) and the position of the mutations identified. The *black* and *white boxes* on genomic DNA (gDNA) denote the coding regions on exons 1-5 (E1-E5) and the untranslated regions, respectively. *OTX2* encodes the HD (a *blue region*), the SIWSPA conserved motif (an *orange region*), and the two tandem tail motifs (*green triangles*). The TD (a *gray triangle*) is assigned to the C-terminal side; deletion of each tail motif reduces the transactivation function, and that of a region distal to the SIWSPA motif further reduces the transactivation function. In addition, another TD may also reside in the 5′ side of the HD (17). The three mutations identified in this study are shown. B, Electrochromatograms showing the mutations in cases 1–4. Shown are the direct sequences and subcloned normal and mutant sequences. The deleted sequences are shaded in *gray*, and the inserted sequence is highlighted in *yellow*. The mutant and the corresponding wild-type nucleotides are indicated by *red asterisks*.

detected by avidin conjugated to fluorescein isothiocyanate. To indicate an extent of a microdeletion, oligoarray comparative genomic hybridization (CGH) was carried out with 1×244K human genome array (catalog no. G4411B; Agilent Technologies, Palo Alto, CA), according to the manufacturer's protocol. Finally, to characterize a microdeletion, long PCR was performed with primer pairs flanking the deleted region, and a long PCR product was subjected to direct sequencing using serial sequence primers. The deletion size and the junction structure were determined by comparing the obtained sequences with the reference sequences at the National Center for Biotechnology Information Database (NC_000014.7; Bethesda, MD), and the presence or absence of repeat sequences around the breakpoints was examined with Repeatmasker (http://www.repeatmasker.org).

Functional studies

Western blot analysis, subcellular localization analysis, DNA binding analysis, and transactivation analysis were performed by the previously reported methods (8) (for details, see Supplemental Methods). In this study, we used the previously reported expression vector and fluorescent vector containing the wild-type *OTX2* cDNA; the probes with the wild-type and mutated OTX2 binding sites within the *IRBP*, *HESX1*, and *POU1F1* promoter sequences; and the luciferase reporter vectors containing the *IRBP*, *HESX1*, and *POU1F1* promoter sequences (8). We further created expression vectors and fluorescent vectors containing mutant *OTX2* cDNAs by site-directed mutagenesis using Prime STAR mutagenesis basal kit (Takara, Otsu, Japan), and constructed a 30-bp probe with wild-type (TAATCT) and mutated (TGGGCT) putative OTX2 binding site within the *GNRH1* promoter sequence and a luciferase reporter vector containing the *GNRH1* promoter sequence (−1349 to −1132 bp) by inserting the corresponding sequence into pGL3 basic. The *GNRH1* promoter sequence was based on the report of Kelley *et al.* (15). Transfections were performed in triplicate within a single experiment, and the experiment was repeated three times.

PCR-based expression analysis of *OTX2*

Human cDNA samples were purchased from CLONTECH (Palo, Alto, CA) except for leukocyte and skin fibroblast cDNA samples that were prepared with Superscript III reverse transcriptase (Invitrogen). PCR amplification was performed for the cDNA samples (0.5 ng), using the primers hybridizing to exon 3 and 4 of *OTX2* and those hybridizing to exons 2/3 and 4/5 (boundaries) of *GAPDH* used as an internal control.

Results

Identification of mutations and substitutions

Three novel heterozygous *OTX2* mutations were identified in four cases, *i.e.* a 16-bp deletion at exon 4 that is predicted to cause a frameshift at the 74th codon for lysine and resultant termination at the 103rd codon (c.221_236del16, p.K74fsX103) in case 1; a 4-bp deletion and a 2-bp insertion at exon 4 that is predicted to cause a frame shift at the 72nd codon for alanine and resultant termination at the 86th codon (c.214_217delGCACinsCA, p.A72fsX86) in case 2; and a nonsense mutation at exon 5 that is predicted to cause a substitution of the 188th glycine with stop codon (c.562G>T, p.G188X) in two unrelated cases (3 and 4; Fig. 1). In addition, heterozygous missense substitutions were identified in patient 1 (c.532A>T, p.T178S) and patient 2 (c.734C>T, p.A245V). Cases 1 and 3 were from group 1, cases 2 and 4 and patient 2 were from group 2, and patient 1 was from group 3. Parental analysis indicated that frameshift mutations in cases 1 and 2 were absent from the parents (*de novo* mutations), whereas the missense substitution of patient 2 was inherited from phenotypically normal father. The parents of cases 3 and 4 and patient 1 refused molecular studies. All the mutations and the missense substitutions were absent from 100 control subjects.

Prediction of the occurrence of aberrant splicing and NMD

The two frameshift mutations and the nonsense mutation were predicted to influence neither exonic splice enhancers nor splice donor and acceptor sites (Supplemental Tables 2 and 3). Furthermore, the two frameshift mutations were predicted to produce the premature termination codons on the mRNA transcribed from the last exon

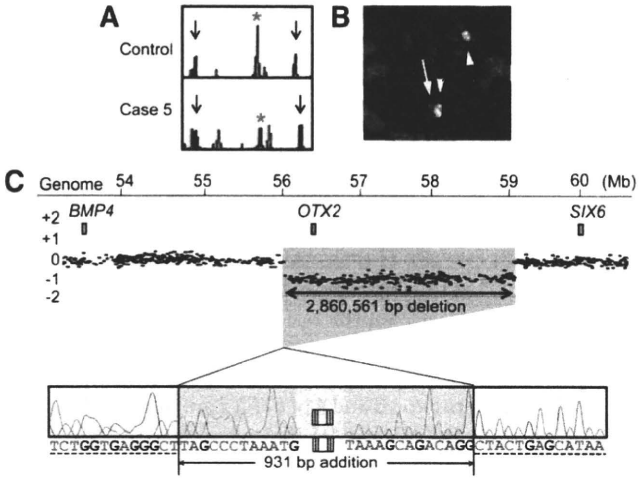

FIG. 2. Deletion analysis in case 5. A, MLPA analysis. The *red asterisk* indicates peaks for the *OTX2* exon 4, and the *black arrows* indicate control peaks. The *red peaks* indicate the internal size markers. Deletion of the MLPA probe binding site is indicated by the reduced peak height. B, FISH analysis. The probe for *OTX2* detects only a *single red signal* (an *arrow*), whereas the RP11-566I2 BAC probe identifies *two green signals* (*arrowheads*). C, Oligoarray CGH analysis and direct sequencing of the deletion junction. The deletion is 2,860,561 bp in physical size (shaded in *gray*) and is associated with an addition of a 931-bp segment (highlighted in *yellow*). The normal sequences flanking the microdeletion are indicated with *dashed underlines*.

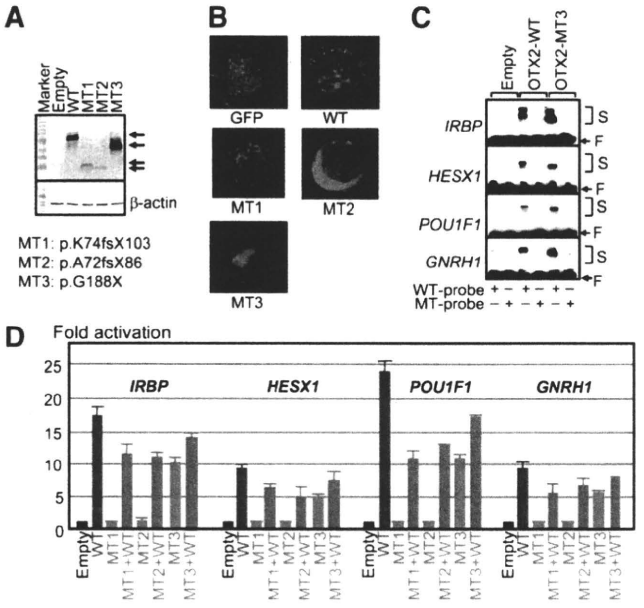

FIG. 3. Functional studies. A, Western blot analysis. Both WT and MT1-MT3 OTX2 proteins are detected with different molecular masses (*arrows*). WT, Wild type; MT1, p.K74fsX103; MT2, p.A72fsX86; and MT3, p.G188X. B, Subcellular localization analysis. Whereas green fluorescent protein (GFP) alone is diffusely distributed throughout the cell, the GFP-fused WT-OTX2 and MT3-OTX2 proteins localize to the nucleus. By contrast, the GFP-fused MT1-OTX2 and MT2-OTX2 proteins are incapable of localizing to the nucleus. C, DNA binding analysis using the wild-type (WT) and mutated (MT) probes derived from the promoters of *IRBP*, *HESX1*, *POU1F1*, and *GNRH1*. The symbols (+) and (−) indicate the presence and absence of the corresponding probes, respectively. Both WT and MT3 OTX2 proteins bind to the WT but not the MT probes. For the probe derived from the *IRBP* promoter, two shifted bands are found for both WT-OTX2 and MT3-OTX2 proteins as reported previously (17). S, Shifted bands; F, free probes. D, Transactivation analysis, using the promoter sequences of *IPBP*, *HESX1*, *POU1F1*, and *GNRH1*. The results are expressed using the mean and SD. The *black*, *blue*, *red*, and *green bars* indicate the data of the empty expression vectors (0.6 μg), expression vectors with WT *OTX2* cDNA (0.6 μg), expression vectors with MT1-MT3 *OTX2* cDNAs (0.6 μg), and the mixture of expression vectors with WT (0.3 μg) and those with MT1-MT3 *OTX2* cDNAs (0.3 μg), respectively; thus, the same amount of expression vectors has been used for each assay.

5, indicating that the frameshift mutations as well as the nonsense mutation had the property to escape NMD (Supplemental Fig. 1).

Identification of a microdeletion

A heterozygous microdeletion affecting *OTX2* was indicated by MLPA and confirmed by FISH in case 5 of group 1 (Fig. 2, A and B). Oligoarray CGH delineated an approximately 2.9-Mb deletion, and sequencing of the fusion point showed that the microdeletion was 2,860,561 bp in physical size (56,006,531–58,867,091 bp on the NC_000014.7) and was associated with an addition of a complex 931-bp segment consisting of the following structures (cen → tel): 2 bp (TA) insertion → 895 bp sequence identical with that in a region just centromeric to the microdeletion (55, 911, 347–55, 912, 241 bp) → 1 bp (C) insertion → 33-bp sequence identical with that within the deleted region (58, 749, 744–58, 749, 776 bp) (Fig. 2C). Repeat sequences were absent around the break points. This microdeletion was not detected in DNA from the parents.

Functional studies of the wild-type and mutant OTX2 proteins

Western blot analysis detected wild-type OTX2 protein of 31.6 kDa and mutant OTX2 proteins of 11.5 kDa (p.K74fsX103), 9.7 kDa (p.A72fsX86), and 15.4 kDa (p.G188X) (Fig. 3A). The molecular masses were as predicted from the mutations. The band intensity was comparable between the wild-type OTX2 protein and the p.G188X-OTX2 protein and was faint for the p.K74fsX103-OTX2 and p.A72fsX86-OTX2 proteins.

Subcellular localization analysis showed that the p.G188X-OTX2 protein localized to the nucleus as did the wild-type OTX2 protein, whereas the p.K74fsX103-OTX2 and p.A72fsX86-OTX2 proteins were incapable of localizing to the nucleus (Fig. 3B). The results were consistent with those of the Western blot analysis because nuclear extracts were used for the Western blotting, with some probable contamination of cytoplasm.

DNA binding analysis revealed that the p.G188X-OTX2 protein with nuclear localizing capacity bound to the wild-type OTX2 binding sites within the four promoters examined, including the *GNRH1* promoter, but not to the mutated OTX2 binding sites (Fig. 3C). The band shift

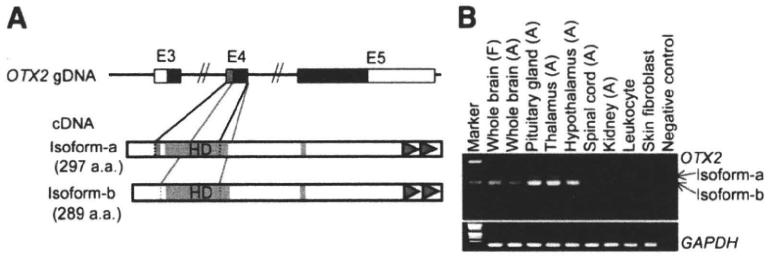

FIG. 4. PCR-based human cDNA library screening for *OTX2* (35 cycles). A, Schematic representation of the *OTX2* isoform-a (NM_21728.2) and isoform-b (NM_172337.1). Because of the two alternative splice acceptor sites at the boundary between intron 3 and exon 4, isoform-a carries eight amino acids (shown in *gray*) in the vicinity of the HD, whereas isoform-b is lacking the eight amino acids. B, PCR amplification data. *OTX2* is clearly expressed in the pituitary and hypothalamus, with isoform-b being the major product. *GAPDH* has been used as an internal control. F, Fetus; A, adult.

was more obvious for the wild-type OTX2 protein than for the p.G188X-OTX2 protein, consistent with the difference in the molecular masses.

Transactivation analysis showed that the wild-type OTX2 protein had transactivation activities for the four promoters examined including the *GNRH1* promoter, whereas the p.K74fsX103-OTX2 and p.A72fsX86-OTX2 proteins had virtually no transactivation function, and the p.G188X-OTX2 protein had reduced (~50%) transactivation activities (Fig. 3D). The three mutant OTX2 proteins had no dominant-negative effects. In addition, the two missense p.A245V-OTX2 and p.T178S-OTX2 proteins had apparently normal transactivation activities with no dominant-negative effect (Supplemental Fig. 2).

PCR-based expression analysis of *OTX2*

OTX2 expression was identified in the pituitary and the hypothalamus as well as in the brain and the thalamus but not detected in the spinal cord, kidney, leukocytes, and skin fibroblasts (Fig. 4). The isoform-b lacking the eight amino acids was predominantly expressed.

Clinical findings in *OTX2* mutation-positive patients

Clinical data are summarized in Table 1 (*left part*). Anophthalmia and/or microphthalmia was present in cases 1–5. Developmental delay was obvious in cases 1 and 3–5, whereas it was obscure in case 2 because of the young age. Prenatal growth was normally preserved in cases 1–5, whereas postnatal growth was compromised in cases 1, 3, and 5. Cases 1 and 5 had IGHD, and case 3 had CPHD (Table 2); furthermore, cases 1, 3, and 5 had pituitary hypoplasia (PH) and/or ectopic posterior pituitary (EPP) (Supplemental Fig. 3). Case 3 showed no pubertal development at 15 yr of age (Tanner pubic hair stage 2 in Japanese boys: 12.5 ± 0.9 yr) (16). Cases 2 and 4 had no discernible pituitary dysfunction and did not receive magnetic resonance imaging examinations. In addition, case 1 had right retractile testis. Patient 1 with p.T178S had CPHD but without ocular anomalies, and patient 2 with p.A245V had bilateral optic nerve hypoplasia and short stature.

Discussion

We identified two frameshift mutations in cases 1 and 2 and a nonsense mutation in unrelated cases 3 and 4. Furthermore, it was predicted that these mutations neither affected splice patterns nor underwent NMD, although direct analysis using mRNA was impossible due to lack of detectable *OTX2* expression in already collected leukocytes as well as skin fibroblasts, which might be available from cases 1–4. Thus, these mutations are predicted to produce aberrant OTX2 proteins *in vivo* that were used in the *in vitro* functional studies. In this context, the functional studies indicated that the two frameshift mutations were amorphic and the nonsense mutation was hypomorphic. The results are consistent with the previous notion that the HD not only has DNA binding capacity but also retains at least a part of nuclear localization signal on its C-terminal portion and the TD primarily resides in the C-terminal region (17) (Fig. 1A). Whereas the two missense substitutions were absent in 100 control subjects, they would be rare normal variations rather than pathological mutations because of the normal transactivation activities with no dominant-negative effect.

We also detected a heterozygous microdeletion involving *OTX2* in case 5 that was not mediated by repeat sequences. This implies the importance of the examination of a microdeletion. Indeed, such a cryptic microdeletion has been identified in multiple genes with the development of MLPA that can serve as a screening method in the detection of microdeletions (18). Whereas the microdeletion of case 5 has removed 16 additional genes (Ensembl Genome Browser, http://www.ensembl.org/), the clinical phenotype of case 5 is explainable by *OTX2* haploinsufficiency alone. Thus, hemizygosity for the 16 genes would not have a major clinical effect, if any.

Furthermore, the present study revealed two findings. First, *OTX2* was expressed in the hypothalamus and had a transactivation function for the *GNRH1* promoter. This implies that *GNRH1* essential for the hypothalamic GnRH secretion is also a target gene of *OTX2*, as has been demonstrated in the mouse (15). Second, the short isoform-b was predominantly identified in the *OTX2* expression-positive tissues. This sug-

TABLE 1. Summary of clinical findings in patients with heterozygous *OTX2* mutations

	Present study					Previous studies[a]			
	Case 1	**Case 2**	**Case 3**	**Case 4**	**Case 5**	**Case 6**	**Case 7**	**Case 8**	**Case 9**
Present age (yr)	3	1	15	10	2	3	6	14	6
Sex	Male	Female	Male	Male	Male	Female	Male	Female	Male
Mutation[b]									
cDNA	c.221_236del	c.214_217del GCACinsCA	c.562G>T	c.562G>T	Whole gene deletion	c.402_403insC	c.674A>G	c.674A>G	c.405_406insCT
Protein	p.K74fsX103	p.A72fsX86	p.G188X	p.G188X	Absent	p. S135fsX136	p.N225S	p.N225S	p.S136fsX178
Function	Severe LOF	Severe LOF	Mild LOF	Mild LOF	Absent	Severe LOF	DN	DN	Severe LOF
Ocular malformation									
Right	AO	MO	MO	MO	MO	AO	N.D.	N.D.	AO
Left	MO	MO	MO	MO	AO	AO	N.D.	N.D.	AO
Developmental delay	+	Uncertain	+	+	+	+	N.D.	N.D.	+
Prenatal growth failure[c]	−	−	−	−	−	−	N.D.	N.D.	−
Birth length (cm) (SDS)	46.5 (−1.2)	48.3 (±0)	50 (+0.5)	49 (±0)	47.9 (−0.5)	50 (+0.6)	N.D.	N.D.	49.5 (+0.2)
Birth weight (kg) (SDS)	2.77 (−0.5)	3.22 (+0.6)	3.62 (+1.5)	3.23 (+0.5)	2.96 (−0.1)	3.16 (+0.2)	N.D.	N.D.	3.49 (+1.2)
Birth OFC (cm) (SDS)	32.5 (−0.7)	34 (+0.7)	N.E.	32.5 (−0.7)	31.5 (−1.4)	33.7 (+0.6)	N.D.	N.D.	N.D.
Postnatal growth failure[c]	+	−	+	−	+	+	+	+	+
Present height (cm) (SDS)	76.9 (−3.3)[d]	73.2 (±0)	114.0 (−4.1)[e]	130.8 (−1.5)	78.1 (−2.4)	85.0 (−3.3)	N.D.	N.D.	81.8 (−5.3)[f]
Present weight (kg) (SDS)	8.9 (−2.6)[d]	8.3 (−0.4)	16.8 (−2.4)[e]	23.2 (−1.6)	9.9 (−1.4)	10.1 (−2.6)	N.D.	N.D.	10.7 (−2.5)[f]
Present OFC (cm) (SDS)	N.E.	N.E.	N.E.	N.E.	N.E.	46 (−1.9)	N.D.	N.D.	47.2 (−2.7)[f]
Paternal height (cm) (SDS)[c]	160 (−1.9)	168 (−0.5)	178 (+1.2)	167 (−0.7)	163 (−1.3)	170 (±0)	178 (+0.3)	188 (+1.8)	N.D.
Maternal height (cm) (SDS)[c]	150 (−1.6)	151 (−1.3)	166 (+1.5)	165 (+1.4)	170 (+2.2)	155 (−0.6)	158 (−0.8)	168 (+0.7)	N.D.
Affected pituitary hormones	GH	No	GH, TSH, PRL, LH, FSH	No	GH	GH	GH, TSH, ACTH, LH, FSH	GH, TSH, ACTH, LH, FSH	GH, TSH, ACTH, LH, FSH
MRI findings									
Pituitary hypoplasia	+	N.E.	+	N.E.	+	−	+	+	+
EPP	+	N.E.	+	N.E.	−	−	+	−	+
Other features	Retractile testis (R)			Seizure		Cleft palate			Chiari malformation

SDS, SD score; OFC, occipitofrontal head circumference; MRI, magnetic resonance imaging; LOF, loss of function; DN, dominant negative; AO, anophthalmia; MO, microphthalmia; N.D., not described; N.E., not examined; PRL, prolactin; R, right.

[a] Case 6, Dateki *et al.* (8); cases 7 and 8, Diaczok *et al.* (9); case 9, Tajima *et al.* (10); [b] the cDNA and protein numbes are based on the human *OTX2* isoform-b (GenBank accession no. NM_172337.1), and the A of the ATG encoding the initiator methionine residue is denoted position +1; thus, the description of the mutations in cases 7–9 is different from that reported by Diaczok *et al.* (9) and Tajima *et al.* (10); [c] assessed by the age- and sex-matched Japanese growth standards (27) (cases 1–6 and 9 and their parents) or by the American growth standards (28) (the parents of cases 7 and 8); [d] at 2 yr 4 months of age before GH treatment; [e] at 10 yr of age before GH treatment; [f] at 4 yr of age before GH treatment.

J Clin Endocrinol Metab, February 2010, 95(2):756–764

TABLE 2. Blood hormone values in cases 1–5 with heterozygous *OTX2* mutations

Patient Sex (age at examination)		Case 1 Male (2 yr)		Case 2 Female (1 yr)		Case 3 Male (14 yr)		Case 4 Male (10 yr)		Case 5 Male (2 yr)	
	Stimulus (dose)	**Basal**	**Peak**	**Basal**	**Peak**	**Basal**	**Peak**	**Basal**	**Peak**	**Basal**	**Peak**
GH (ng/ml)	Insulin (0.1 U/kg)[a]	1.9[b]	**4.0**[b]	3.3[b]	N.E.	0.8[b]	**1.3**[b]	12.1[b]	N.E.	0.5[c]	**9.0**[c]
	Arginine (0.5 g/kg)									1.1[c]	**7.0**[c]
	L-dopa (10 mg/kg)	1.5[b]	**3.8**[b]			0.3[b]	**1.0**[b]				
LH (mIU/ml)	GnRH (100 $\mu g/m^2$)	0.1	1.7	0.1	N.E.	2.3[d]	**4.5**	0.4	N.E.	0.1	3.1
FSH (mIU/ml)	GnRH (100 $\mu g/m^2$)	1.0	6.2	3.7	N.E.	1.3[d]	**6.3**	1.1	N.E.	1.5	9.9
TSH (μU/ml)	TRH (10 μg/kg)	4.2	23.8	1.1	N.E.	0.2	**1.9**	1.1	N.E.	5.2	19.5
Prolactin (ng/ml)	TRH (10 μg/kg)	17.9	34.5	N.E.	N.E.	5.5	**8.3**	9.1	N.E.	10.43	88.8
ACTH (pg/ml)	Insulin (0.1 U/kg)	31	195	N.E.	N.E.	24		N.E.	N.E.	41	222
Cortisol (μg/dl)[d]	Insulin (0.1 U/kg)	12.7		9.4	N.E.	19.4		N.E.	N.E.	25.4	39.2
IGF-I (ng/ml)		**8**		65	N.E.	**5**		214	N.E.	48	
Testosterone (ng/dl)		N.E.		N.E.	N.E.	**45**		<5	N.E.	N.E.	
Free T_4 (ng/dl)		1.32		1.17	N.E.	**0.87**		1.15	N.E.	1.17	
Free T_3 (pg/ml)		2.91		3.24	N.E.	**1.94**		3.92	N.E.	4.54	

The conversion factor to the SI unit: GH, 1.0 (μg/liter); LH, 1.0 (IU/liter); FSH, 1.0 (IU/liter); TSH, 1.0 (mIU/liter); prolactin, 1.0 (μg /liter); ACTH, 0.22 (pmol/liter); cortisol, 27.59 (nmol/liter); IGF-I, 0.131 (nmol/liter); testosterone, 0.035 (nmol/liter); free T_4, 12.87 (pmol/liter); and free T_3, 1.54 (pmol/liter). Hormone values have been evaluated by the age- and sex-matched Japanese reference data (29, 30); low hormone data are *boldfaced*. Blood sampling during the provocation tests: 0, 30, 60, 90, and 120 min. N.E., Not examined.

[a] Sufficient hypoglycemic stimulations were obtained during all the insulin provocation tests; [b] GH was measured using the recombinant GH standard, and the peak GH values of 6 and 3 ng/ml are used as the cutoff values for partial and severe GH deficiency, respectively; [c] GH was measured by the classic RIA, and the peak GH values of 10 and 5 ng/ml were used as the cutoff values for partial and severe GH deficiency; [d] Obtained at 0800–0900 h.

gests that the biological functions of *OTX2* are primarily contributed by the short isoform-b.

Clinical features of cases 1–5 are summarized in Table 1, together with those of the previously reported *OTX2* mutation-positive patients examined for detailed pituitary function. Here four patients with cytogenetically recognizable deletions involving *OTX2* are not included (19–22) because the deletions appear to have removed a large number of genes including *BMP4* and/or *SIX6* (Fig. 2B) that can be relevant to pituitary development and/or function (1, 23).

Several points are noteworthy for the clinical findings. First, although cases 1–5 in this study had anophthalmia and/or microphthalmia, ocular phenotype has not been described in cases 7 and 8 identified by *OTX2* mutation analysis in 50 patients with hypopituitarism (9). Whereas no description of a phenotype would not necessarily indicate the lack of the phenotype, *OTX2* mutations may specifically affect pituitary function at least in several patients. This would not be unexpected because several *OTX2* mutation-positive patients are free from ocular anomalies (6).

Second, pituitary phenotype is variable and independent of the *in vitro* function data. This would be explained by the notion that haploinsufficiency of developmental genes is usually associated with a wide range of penetrance and expressivity depending on other genetic and environmental factors (24), although the actual underlying factors remain to be identified. In this regard, because direct mRNA analysis was not performed, it might be possible that the mutations have not produced the predicted aberrant protein and, consequently, *in vitro* function data do not necessarily reflect the *in vivo* functions. Even if this is the case, the quite different pituitary phenotype between cases 3 and 4 with the same mutation would argue for the notion that pituitary phenotype is independent of the residual OTX2 function.

Third, cases 1, 3, 5, and 6–9 with pituitary dysfunction have IGHD or CPHD involving GH, and show the combination of preserved prenatal growth and compromised postnatal growth characteristic of GH deficiency (25). This suggests that GH is the most vulnerable pituitary hormone in *OTX2* mutations. Consistent with this, previously reported patients with ocular anomalies and *OTX2* mutations also frequently exhibit short stature (6, 8). Thus, pituitary function studies are recommended in patients with ocular anomalies and postnatal short stature to allow for appropriate hormone therapies including GH treatment for short stature, cortisol supplementation at a stress period, T_4 supplementation to protect the developmental deterioration, and sex steroid supplementation to induce secondary sexual characteristics. Furthermore, *OTX2* mutation analysis is also recommended in such patients.

Lastly, PH and/or EPP is present in patients with IGHD and CPHD, except for case 6 with IGHD. In this regard, the following findings are noteworthy: 1) heterozygous loss-of-function mutations of *HESX1* are associated with a wide phenotypic spectrum including CPHD, IGHD, and apparently normal phenotype and often cause PH and

EPP, whereas homozygous *HESX1* mutations usually lead to CPHD as well as PH and EPP (2); 2) heterozygous loss-of-function mutations of *POU1F1* usually permit apparently normal pituitary phenotype, whereas homozygous loss-of-function mutations and heterozygous dominant-negative mutations usually result in GH, TSH, and prolactin deficiencies and often cause PH but not EPP (2); and 3) heterozygous *GNRH1* frameshift mutation are free from discernible phenotype, whereas homozygous *GNRH1* mutations result in isolated hypogonadotropic hypogonadism with no abnormal pituitary structure (26). Collectively, overall pituitary phenotype may primarily be ascribed to reduced *HESX1* expression, although reduced *POU1F1* and *GNRH1* expressions would also play a certain role, and there may be other target genes of *OTX2*.

In summary, the results imply that *OTX2* mutations are associated with variable pituitary phenotype, with no genotype-phenotype correlations, and that *OTX2* can transactivate *GNRH1* as well as *HESX1* and *POU1F1*. Further studies will serve to clarify the role of *OTX2* in the pituitary development and function.

Acknowledgments

We thank the patients and parents for participating in this study. We also thank Dr. Nicola Ragge and Dr. David J Bunyan for the MLPA probe sequence of *OTX2*.

Address all correspondence and requests for reprints to: Dr. T. Ogata, Department of Endocrinology and Metabolism, National Research Institute for Child Health and Development, 2-10-1 Ohkura, Setagaya, Tokyo 157-8535, Japan. E-mail: tomogata@nch.go.jp.

This work was supported by Grants-in-Aid for Young Scientists (B-21791025) from the Ministry of Education, Culture, Sports, Science, and Technology and Grants for Child Health and Development (20C-2); Research on Children and Families (H21-005); and Research on Measures for Intractable Diseases (H21-043) from the Ministry of Health, Labor, and Welfare.

Disclosure Summary: The authors have nothing to declare.

References

1. **Cohen LE, Radovick S** 2002 Molecular basis of combined pituitary hormone deficiencies. Endocr Rev 23:431–442
2. **Kelberman D, Dattani MT** 2007 Hypopituitarism oddities: congenital causes. Horm Res 68(Suppl 5):138–144
3. **Vieira TC, Boldarine VT, Abucham J** 2007 Molecular analysis of PROP1, PIT1, HESX1, LHX3, and LHX4 shows high frequency of PROP1 mutations in patients with familial forms of combined pituitary hormone deficiency. Arq Bras Endocrinol Metab 51:1097–1103
4. **Hever AM, Williamson KA, van Heyningen V** 2006 Developmental malformations of the eye: the role of *PAX6*, *SOX2* and *OTX2*. Clin Genet 69:459–470
5. **Courtois V, Chatelain G, Han ZY, Le Novère N, Brun G, Lamonerie T** 2003 New Otx2 mRNA isoforms expressed in the mouse brain. J Neurochem 84:840–853
6. **Ragge NK, Brown AG, Poloschek CM, Lorenz B, Henderson RA, Clarke MP, Russell-Eggitt I, Fielder A, Gerrelli D, Martinez-Barbera JP, Ruddle P, Hurst J, Collin JR, Salt A, Cooper ST, Thompson PJ, Sisodiya SM, Williamson KA, Fitzpatrick DR, van Heyningen V, Hanson IM** 2005 Heterozygous mutations of *OTX2* cause severe ocular malformations. Am J Hum Genet 76:1008–1022
7. **Wyatt A, Bakrania P, Bunyan DJ, Osborne RJ, Crolla JA, Salt A, Ayuso C, Newbury-Ecob R, Abou-Rayyah Y, Collin JR, Robinson D, Ragge N** 2008 Novel heterozygous OTX2 mutations and whole gene deletions in anophthalmia, microphthalmia and coloboma. Hum Mutat 29:E278–E283
8. **Dateki S, Fukami M, Sato N, Muroya K, Adachi M, Ogata T** 2008 OTX2 mutation in a patient with anophthalmia, short stature, and partial growth hormone deficiency: functional studies using the IRBP, HESX1, and POU1F1 promoters. J Clin Endocrinol Metab 93:3697–3702
9. **Diaczok D, Romero C, Zunich J, Marshall I, Radovick S** 2008 A novel dominant-negative mutation of OTX2 associated with combined pituitary hormone deficiency. J Clin Endocrinol Metab 93:4351–4359
10. **Tajima T, Ohtake A, Hoshino M, Amemiya S, Sasaki N, Ishizu K, Fujieda K** 2009 OTX2 loss of function mutation causes anophthalmia and combined pituitary hormone deficiency with a small anterior and ectopic posterior pituitary. J Clin Endocrinol Metab 94:314–319
11. **Cartegni L, Chew SL, Krainer AR** 2002 Listening to silence and understanding nonsense: exonic mutations that affect splicing. Nat Rev Genet 3:285–298
12. **Strachan T, Read AP** 2004 Instability of the human genome: mutation and DNA repair. In: Human molecular genetics. 3rd ed. London and New York: Garland Science; 334–337
13. **Holbrook JA, Neu-Yilik G, Hentze MW, Kulozik AE** 2004 Nonsense-mediated decay approaches the clinic. Nat Genet 36:801–808
14. **Schouten JP, McElgunn CJ, Waaijer R, Zwijnenburg D, Diepvens F, Pals G** 2002 Relative quantification of 40 nucleic acid sequences by multiplex ligation-dependent probe amplification. Nucleic Acids Res 30:e57
15. **Kelley CG, Lavorgna G, Clark ME, Boncinelli E, Mellon PL** 2000 The Otx2 homeoprotein regulates expression from the gonadotropin-releasing hormone proximal promoter. Mol Endocrinol 14:1246–1256
16. **Matsuo N** 1993 Skeletal and sexual maturation in Japanese children. Clin Pediatr Endocrinol 2(Suppl):1–4
17. **Chatelain G, Fossat N, Brun G, Lamonerie T** 2006 Molecular dissection reveals decreased activity and not dominant-negative effect in human OTX2 mutants. J Mol Med 84:604–615
18. **den Dunnen JT, White SJ** 2006 MLPA and MAPH: sensitive detection of deletions and duplications. Curr Protoc Hum Genet Chapter 7, Unit 7.14
19. **Bennett CP, Betts DR, Seller MJ** 1991 Deletion 14q (q22q23) associated with anophthalmia, absent pituitary, and other abnormalities. J Med Genet 28:280–281
20. **Elliott J, Maltby EL, Reynolds B** 1993 A case of deletion 14(q22.1→q22.3) associated with anophthalmia and pituitary abnormalities. J Med Genet 30:251–252
21. **Lemyre E, Lemieux N, Décarie JC, Lambert M** 1998 Del(14)(q22.1q23.2) in a patient with anophthalmia and pituitary hypoplasia. Am J Med Genet 77:162–165
22. **Nolen LD, Amor D, Haywood A, St Heaps L, Willcock C, Mihelec M, Tam P, Billson F, Grigg J, Peters G, Jamieson RV** 2006 Deletion at 14q22–23 indicates a contiguous gene syndrome comprising anophthalmia, pituitary hypoplasia, and ear anomalies. Am J Med Genet A 140:1711–1718

23. **Zhu X, Lin CR, Prefontaine GG, Tollkuhn J, Rosenfeld MG** 2005 Genetic control of pituitary development and hypopituitarism. Curr Opin Genet Dev 15:332–340
24. **Fisher E, Scambler P** 1994 Human haploinsufficiency— one for sorrow, two for joy. Nat Genet 7:5–7
25. **Parks JS, Felner EI** 2007 Hypopituitarism. In: Kliegman RM, Behrman RE, Jenson HB, Stanton BF, eds. Nelson textbook of pediatrics. 18th ed. Philadelphia: Saunders Elsevier; 2293–2299
26. **Bouligand J, Ghervan C, Tello JA, Brailly-Tabard S, Salenave S, Chanson P, Lombès M, Millar RP, Guiochon-Mantel A, Young J** 2009 Isolated familial hypogonadotropic hypogonadism and a GNRH1 mutation. N Engl J Med 360:2742–2748
27. **Suwa S, Tachibana K, Maesaka H, Tanaka T, Yokoya S** 1992 Longitudinal standards for height and height velocity for Japanese children from birth to maturity. Clin Pediatr Endocrinol 1:5–13
28. **Kuczmarski RJ, Ogden CL, Guo SS, Grummer-Strawn LM, Flegal KM, Mei Z, Wei R, Curtin LR, Roche AF, Johnson CL** 2002 2000 CDC growth charts for the United States: methods and development. Vital Health Stat 11 246:1–190
29. **Japan Public Health Association** 1996 Normal biochemical values in Japanese children (in Japanese). Tokyo: Sanko Press
30. **Inada H, Imamura T, Nakajima R** 2002 Manual of endocrine examination for children (in Japanese). Osaka: Medical Review

Mutation and Gene Copy Number Analyses of Six Pituitary Transcription Factor Genes in 71 Patients with Combined Pituitary Hormone Deficiency: Identification of a Single Patient with *LHX4* Deletion

Sumito Dateki, Maki Fukami, Ayumi Uematsu, Masayuki Kaji, Manami Iso, Makoto Ono, Michiyo Mizota, Susumu Yokoya, Katsuaki Motomura, Eiichi Kinoshita, Hiroyuki Moriuchi, and Tsutomu Ogata

Department of Endocrinology and Metabolism (S.D., M.F., M.I., T.O.), National Research Institute for Child Health and Development, Tokyo 157-8535, Japan; Department of Pediatrics (S.D., K.M., E.K., H.M.), Nagasaki University Graduate School of Biomedical Sciences, Nagasaki 852-8501, Japan; Division of Endocrinology and Metabolism (A.U., M.K), Shizuoka Children's Hospital, Shizuoka 232-8555, Japan; Department of Pediatrics and Developmental Biology (M.O.), Tokyo Medical and Dental University Graduate School of Medical and Dental Sciences, Tokyo 113-8519, Japan; Department of Pediatrics (M.M.), Faculty of Medicine, Kagoshima University, Kagoshima 890-8544, Japan; Department of Medical Subspecialties (S.Y.), National Children's Medical Center, Tokyo 157-8535, Japan

Context: Mutations of multiple transcription factor genes involved in pituitary development have been identified in a minor portion of patients with combined pituitary hormone deficiency (CPHD). However, copy number aberrations involving such genes have been poorly investigated in patients with CPHD.

Objective: We aimed to report the results of mutation and gene copy number analyses in patients with CPHD.

Subjects and Methods: Seventy-one Japanese patients with CPHD were examined for mutations and gene copy number aberrations affecting *POU1F1*, *PROP1*, *HESX1*, *LHX3*, *LHX4*, and *SOX3* by PCR-direct sequencing and multiplex ligation-dependent probe amplification. When a deletion was indicated, it was further studied by fluorescence *in situ* hybridization, oligoarray comparative genomic hybridization, and serial sequencing for long PCR products encompassing the deletion junction.

Results: We identified a *de novo* heterozygous 522,009-bp deletion involving *LHX4* in a patient with CPHD (GH, TSH, PRL, LH, and FSH deficiencies), anterior pituitary hypoplasia, ectopic posterior pituitary, and underdeveloped sella turcica. We also identified five novel heterozygous missense substitutions (p.V201I and p.H387P in *LHX4*, p.T63M and p.A322T in *LHX3*, and p.V53L in *SOX3*) that were assessed as rare variants by sequencing analyses for control subjects and available parents and by functional studies and *in silico* analyses.

Conclusions: The results imply the rarity of abnormalities affecting the six genes in patients with CPHD and the significance of the gene copy number analysis in such patients. (***J Clin Endocrinol Metab* 95: 4043–4047, 2010**)

ISSN Print 0021-972X ISSN Online 1945-7197
Printed in U.S.A.

doi: 10.1210/jc.2010-0150 Received January 20, 2010. Accepted May 13, 2010.
First Published Online June 9, 2010

Abbreviations: CGH, Comparative genomic hybridization, CPHD, combined pituitary hormone deficiency, ESE, exonic splice enhancer, FISH, fluorescence *in situ* hybridization, HPA, hypothalamic-pituitary-adrenal, MLPA, multiplex ligation-dependent probe amplification

Pituitary development and function depends on spatially and temporally controlled expression of multiple transcription factor genes such as *POU1F1*, *PROP1*, *HESX1*, *LHX3*, *LHX4*, *SOX3*, and *OTX2* (1–3). Mutations of these genes are usually associated with combined pituitary hormone deficiency (CPHD), although they sometimes lead to isolated GH deficiency (1–3). However, mutations of these genes have been found only in a minor portion of patients with CPHD (2–6). Thus, although multiple genes would remain to be identified in CPHD, a certain fraction of mutations may have been overlooked in these known genes. In this regard, because previous studies have primarily been performed with PCR-direct sequencing for coding exons (4–6), gene copy number aberrations (deletions and duplications) affecting such genes, as well as pathological mutations in noncoding regions, may remain undetected in patients with CPHD. Indeed, microdeletions of *PROP1* and *LHX3* and microduplications of *SOX3* have been identified in a few patients with CPHD (7–9). Thus, we performed sequence and gene copy number analyses for six pituitary transcription factor genes in Japanese patients with CPHD.

Patients and Methods

Patients

We studied 71 Japanese patients with various types of CPHD (39 males and 32 females; age 1–43 yr). In all the patients, *OTX2* mutations and gene copy number aberrations have been excluded previously (3).

Primers and probes

The primers and probes used are summarized in Supplemental Table 1 (published on The Endocrine Society's Journals Online web site at http://jcem.endojournals.org).

Sequence analysis

This study was approved by the Institutional Review Board Committee at the National Center for Child Health and Development. After obtaining written informed consent, leukocyte genomic DNA samples of the 71 patients were amplified by PCR for the all coding exons and their flanking splice sites of *POU1F1*, *PROP1*, *HESX1*, *LHX3*, *LHX4*, and *SOX3*. Subsequently, the PCR products were subjected to direct sequencing on a CEQ 8000 autosequencer (Beckman Coulter, Fullerton, CA). To confirm a heterozygous substitution, the corresponding PCR products were subcloned with a TOPO TA cloning kit (Invitrogen, Carlsbad, CA), and normal and mutant alleles were sequenced separately. The GenBank sequence data at NCBI (http://www.ncbi.nlm.nih.gov/genbank) were used as references. For controls, DNA samples of 100 Japanese healthy adults were used with permission.

Functional studies

Functional studies were performed for an *LHX4* missense variant (for details, see Supplemental Methods). In brief, we constructed expression vectors containing wild-type and variant *LHX4* cDNAs and a luciferase reporter vector containing the *POU1F1* promoter sequence with an LHX4-binding site (10). Subsequently, transactivation analysis was performed with dual-luciferase reporter assay system (Promega, Madison, WI) using COS1 cells.

In silico analyses

The conservation status of substituted wild-type amino acid residues was investigated using the UniGene data at NCBI. The possibility that identified substitutions could cause aberrant splicing was examined by ESE finder release 3.0 for the prediction of exonic splice enhancers (ESEs) (http://rulai.cshl.edu/cgi-bin/tools/ESE3/esefinder.cgi) (11) and by the program at Berkeley *Drosophila* Genome Project for the prediction of splice donor and accepter sites (http://www.fruitfly.org/seq_tools/splice.html) (12).

Gene copy number analysis

Muitlplex ligation-dependent probe amplification (MLPA) (13) was performed as a screening of a possible gene copy number alteration (deletion and duplication) in all 71 patients, using a commercially available MLPA probe mix (P236) (MRC-Holland, Amsterdam, The Netherlands) for all coding exons of *POU1F1*, *PROP1*, *HESX1*, *LHX3*, and *LHX4*, together with originally designed probes for *SOX3*. The procedure was as described in the manufacturer's instructions. To confirm a deletion, fluorescence *in situ* hybridization (FISH) was performed with a long PCR product. To indicate an extent of a deletion, oligoarray comparative genomic hybridization (CGH) was carried out with 1x244K Human Genome Array (catalog no. G4411B; Agilent Technologies, Santa Clara, CA), according to the manufacturer's protocol. Finally, to characterize a deletion, long PCR was performed with primer pairs flanking the deleted region, and the PCR product was subjected to direct sequencing using serial sequence primers. The deletion size and the junction structure were determined by comparing the obtained sequences with the reference sequences at NCBI Database (NC_000014.7), and additional deleted genes were examined with Ensembl Database (http://www.ensembl.org/). The presence or absence of repeat sequences around the breakpoints was examined with Repeatmasker (http://www.repeatmasker.org).

Results

Identification of five missense variants

We identified five novel heterozygous missense substitutions, *i.e.* p.T63M (c.188C→T) and p.A322T (c.964G→A) in *LHX3* (GenBank accession number NM_178138), p.V201I (c.601G→A) and p.H387P (c.1160A→C) in *LHX4* (NM_033343), and p.V53L (c.157G→C) in *SOX3* (NM_005634). These substitutions were found in different patients. No other mutations or novel substitutions were identified in the six genes examined. In the 100 control subjects, *LHX4*-p.H387P was detected in four subjects and *SOX3*-p.V53L in three subjects, whereas *LHX3*-p.T63M, *LHX3*-p.A322T, and *LHX4*-p.V201I were absent. Furthermore, sequencing of